NACA RM L51F06

NACA

RESEARCH MEMORANDUM

EXPLORATORY INVESTIGATION AT HIGH AND LOW SUBSONIC MACH NUMBERS OF TWO EXPERIMENTAL 6-PERCENT-THICK AIRFOIL SECTIONS DESIGNED TO HAVE HIGH MAXIMUM LIFT COEFFICIENTS

By Laurence K. Loftin, Jr., and Albert E. von Doenhoff

Langley Aeronautical Laboratory
Langley Field, Va.

NATIONAL ADVISORY COMMITTEE FOR AERONAUTICS

WASHINGTON

December 14, 1951
Declassified July 29, 1954

NATIONAL ADVISORY COMMITTEE FOR AERONAUTICS

RESEARCH MEMORANDUM

EXPLORATORY INVESTIGATION AT HIGH AND LOW SUBSONIC MACH NUMBERS OF TWO EXPERIMENTAL 6-PERCENT-THICK AIRFOIL SECTIONS DESIGNED TO HAVE HIGH MAXIMUM LIFT COEFFICIENTS

By Laurence K. Loftin, Jr., and Albert E. von Doenhoff

SUMMARY

An investigation has been made to determine whether thin airfoils, which have increased values of the low-speed maximum lift coefficient but which at the same time retain the basic advantages of thin sections at high Mach numbers, can be developed. Airfoil data, which are available in the literature, were analyzed and an approximate relation between the airfoil pressure distribution and the maximum lift coefficient was found. With the use of this relation as a guide, several experimental thin airfoil sections having pressure distributions favorable for high maximum lift coefficients were derived. Two of these airfoil sections which were symmetrical and 6 percent thick have been investigated at both high and low subsonic Mach numbers.

Both of the two new sections had low-speed maximum lift coefficients of about 1.3 at a Reynolds number of 9.0×10^6 as compared to values of about 0.8 which are characteristic of other 6-percent-thick symmetrical airfoil sections. No significant differences in the lift and moment characteristics of the new airfoils as compared to the NACA 64-006 airfoil section were found at high Mach numbers, at least through most of the limited angle-of-attack range of the present investigation. (Maximum angle of attack for the high-speed tests was 6°.) The drag divergence Mach numbers of the new sections were lower than those of the NACA 64-006. The data for the two new sections, however, indicate the possibility that other airfoils can be designed which have increased values of the drag-divergence Mach number with but little decrease in the low-speed maximum lift coefficient.

INTRODUCTION

Various experimental investigations have shown that extremely thin airfoil sections have many aerodynamic advantages at high subsonic and transonic Mach numbers. One of the disadvantages of such sections, however, is their very low maximum lift coefficients at low speeds corresponding to the landing condition of high-speed aircraft. For example, all 6-percent-thick symmetrical airfoil sections for which data are available have low-speed maximum lift coefficients of the order of 0.8 to 0.9 regardless of surface condition for Reynolds numbers less than 20 to 25 $\times 10^6$ (references 1 and 2).

An investigation has been undertaken in an effort to determine whether thin symmetrical airfoils, which would have maximum lift coefficients substantially greater than 0.8 but which would, at the same time, have high-speed characteristics as good as those of thin airfoils of conventional design, could be developed. As a result of this investigation, two experimental symmetrical airfoils of 6-percent thickness have been derived and tested in two-dimensional flow at both high and low Mach numbers. The methods by which the airfoils were derived and the test results obtained are presented and discussed in the present paper.

SYMBOLS

x	distance along chord
y	distance normal to chord
t	airfoil maximum thickness
c	chord
α_o	section angle of attack
c_l	section lift coefficient
c_{l_i}	section design lift coefficient
$c_{l_{max}}$	section maximum lift coefficient
c_d	section drag coefficient

$c_{m_{c/4}}$	section pitching-moment coefficient about quarter chord
$c_{m_{ac}}$	section pitching-moment coefficient about aerodynamic center
R	Reynolds number based on wing chord and free-stream velocity
R'	unit Reynolds number based on free-stream velocity and a length of 1 foot
M_o	free-stream Mach number
p_s	stagnation pressure
p_i	minimum static pressure near leading edge at $c_{l_{max}} - 0.1$
p_2	static pressure at 0.9c station at $c_{l_{max}} - 0.1$
q_1	maximum dynamic pressure near leading edge at $c_{l_{max}} - 0.1$
p_o	free-stream static pressure
q_o	free-stream dynamic pressure
S	pressure coefficient $\left(\frac{p_s - p_o}{q_o}\right)$
V	free-stream velocity
v	local velocity
Δv_a	local velocity increment due to angle of attack
A_1, A_2	airfoil design constants
ϕ	angular coordinate of true circle plane (reference 6)
ψ	airfoil design parameter (reference 6)
ψ_{LE}	value of ψ at leading edge

DERIVATION OF AIRFOIL SECTIONS

Correlation of maximum lift coefficient with pressure distribution.- The stall of an airfoil section is believed to be involved with the behavior of the so-called "laminar separation bubble" near the leading edge and with the behavior of the turbulent boundary layer following reattachment of the separated layer just behind the leading edge (references 2 and 3). An understanding of these phenomena sufficiently detailed to permit an exact calculation of the maximum lift coefficient for a given pressure distribution and Reynolds number, however, has not been reached at the present time. For this reason, an approximate method for estimating the effect of airfoil section on the maximum lift coefficient has been developed. It should perhaps be pointed out in the beginning that this method most certainly cannot be justified from first principles; however, it did seem to offer at least a rough guide to the manner in which a thin airfoil should be designed to give a high maximum lift coefficient.

The method developed is based on the fundamental assumption that the stall at maximum lift results primarily from separation of the turbulent boundary layer and that for purposes of analysis, the boundary layer at high-lift coefficients may be considered turbulent from the point of minimum pressure near the leading edge to the trailing edge. These assumptions would be expected to apply only in the range of Reynolds number in which the maximum lift of smooth airfoils does not vary to any large extent. The assumptions are, of course, more nearly correct for airfoils in the rough surface condition since in this case the boundary layer is turbulent over the entire airfoil surface at all Reynolds numbers. An empirical method developed by von Doenhoff and Tetervin (reference 4) permits the determination of the turbulent boundary-layer separation point from a knowledge of the pressure distribution, wall shear, and turbulent boundary-layer shape and thickness at the point of application of the adverse gradient. Use of this method has indicated that for a given boundary-layer shape at the point of application of the adverse gradient, separation of the turbulent layer is primarily related to the amount of static pressure recovery and is only secondarily dependent upon the detailed shape of the pressure distribution and upon the Reynolds number. The shape of the pressure distribution and the shape of the turbulent boundary-layer velocity profile at or near the point of minimum pressure would not be expected to vary much for different airfoils near maximum lift. Consequently, it seemed reasonable that separation corresponding to the occurrence of the maximum lift coefficient of various airfoils should occur, to the first order at least, at a relatively constant value of the difference

between the minimum static pressure near the leading edge and the static pressure at the separation point near the trailing edge. This pressure difference can be expressed in the form $\frac{p_2 - p_1}{q_1}$ where p_1 and q_1 are the static and dynamic pressures at the minimum point near the leading edge and p_2 is the pressure in the vicinity of the separation point near the trailing edge.

An examination of lift data for a large number of airfoils indicated that the curve of lift coefficient against angle of attack is usually essentially linear until a lift coefficient of about 0.1 less than the maximum is reached. It was assumed that at a lift coefficient of 0.1 less than the maximum, the separation point was between the 90- and 100-percent-chord stations and that further increases in angle of attack caused a rapid forward movement of the separation point. The value of the parameter $\frac{p_2 - p_1}{q_1}$, where p_1 is the minimum pressure near the leading edge and p_2 is the pressure at the 90-percent-chord station, evaluated at a lift coefficient of 0.1 less than the maximum, was taken to be indicative of critical conditions necessary for the complete separation corresponding to maximum lift.

In order to check the validity of the assumptions involved in the method and to determine the value of the critical pressure recovery parameter, should one exist, the value of $\frac{p_2 - p_1}{q_1}$ at $c_{l_{max}} - 0.1$ was evaluated for approximately 45 airfoils, both cambered and uncambered and in both the smooth and rough surface conditions. The lift data were obtained from reference 1 and were for a Reynolds number of 6.0×10^6. The values of the pressure-recovery parameter at this lift coefficient were determined from the theoretical pressure-distribution data of reference 1. It is, of course, recognized that there are differences in the theoretical and actual pressure distributions about airfoil sections, particularly at high lift coefficients. Because of the lack of experimental pressure-distribution data for large numbers of airfoils, however, it was necessary to use the theoretical data. The range of thickness ratio investigated was from 8 to 15 percent chord. Airfoils less than 8 percent in thickness were not considered because detailed surface pressure and boundary-layer measurements on a 6-percent-thick airfoil (reference 5) indicate that, even at relatively low lift coefficients, the experimental pressure distribution near the leading

edge bears little resemblance to the theoretical distribution and that large regions of local separation which may extend as far back from the leading edge as 50-percent chord exist near maximum lift. This type of flow field which is basically different from that of thicker airfoils near maximum lift violates the assumptions of the method. Airfoils greater than 15 percent in thickness ratio were not considered because the maximum lift coefficient of such airfoils in the smooth condition generally varies rather rapidly with Reynolds number for values of the order of 6.0×10^6, and hence, the assumptions of the method would be violated.

The pressure-recovery parameter is plotted against $c_{l_{max}} - 0.1$ for the smooth airfoils in figure 1(a) and for the rough airfoils in figure 1(b). Although there is some scatter in the data, the correlation seems rather good in view of the relatively crude nature of the analysis. There is some indication that the critical pressure-recovery parameter decreases somewhat with increasing lift coefficient, particularly for the rough surface condition. This trend, however, is not very well defined and in accordance with the assumptions of the analysis, the data are interpreted as yielding two constant values of the critical pressure-recovery parameter for the smooth and rough surface conditions, respectively.

Specification of airfoil shape.- With the correlation presented in figure 1, the problem of designing a thin airfoil to have a particular maximum lift coefficient resolves itself into the determination of that airfoil shape for which the critical value of the pressure-recovery parameter will be reached at a lift coefficient 0.1 below the desired maximum value. The potential theory of airfoil sections of arbitrary shape developed by Theodorsen and Garrick (reference 6) provides a means for the direct calculation of the pressure distribution of an airfoil of given shape, and by a series of successive applications of the method, an airfoil shape may be derived to have a specified pressure distribution. This latter process is tedious and time-consuming at best and is extremely difficult if not impossible for the solution of the problem of determining a shape to have a prescribed value of the pressure near the leading edge at a particular lift coefficient. Consequently, a procedure somewhat different from that of deriving an airfoil section to have a specified pressure distribution was employed in the present case.

In the theory of Theodorsen and Garrick, the airfoil ordinates and pressure distribution are related in a rather complicated fashion

to two mutually dependent parameters, ψ and ϵ, which characterize the transformation of an airfoil to a circle. The absolute value of ψ at a particular point on the airfoil is a measure of its thickness and the distribution of ψ is related to the airfoil thickness distribution and to the pressure distribution. In the present investigation, the parameter ψ was expressed as a function containing two arbitrary constants. The form of the function, which is given by the following expression

$$\psi = A_1 \left\{ 1 + \cos\left[1 + \frac{A_2}{2}(1 + \cos \phi) \right] \phi \right\} \qquad (1)$$

is such that by increasing A_2, while adjusting A_1 to maintain a constant thickness ratio, the value of ψ in the vicinity of the leading edge increases thus making the leading edge more bulbous and reducing the values of the peak negative pressure coefficient near the leading edge at high lift coefficients. The variable ϕ in equation (1) is the angular coordinate in the true circle plane of reference 6. Equation (1) can be used with values of A_2 varying from 0 to 2.0. For values of A_2 greater than 2.0, the values of ψ near the leading edge ($\phi = 0$ corresponds to leading-edge point) decrease and the distribution of ψ as a function of ϕ shows some undesirable peaks.

Airfoils of 6-percent thickness were derived for ψ distributions determined by values of A_2 varying from 0 to 1.6. The ψ distributions adjusted to a thickness ratio of 6 percent for the different values of A_2 are shown in figure 2. It can be seen that as A_2 increases, the values of ψ in the vicinity of the leading edge increase quite rapidly while those over the rear part of the airfoil decrease.

Effect of leading-edge shape on pressure distribution and maximum lift.- The pressure-recovery parameter $\frac{p_2 - p_1}{q_1}$ is plotted in figure 3 as a function of lift coefficient for the airfoils having various values of ψ_{LE}. The two horizontal lines in figure 3 represent the critical values of the pressure-recovery parameter as determined from figure 1 for the airfoils smooth and rough. Presumably, the intersections of the curves of pressure recovery parameter against lift coefficient with the horizontal lines representing the critical value of the pressure-recovery parameter are indicative of the values of $c_{l_{max}} - 0.1$ which can be obtained by the different airfoils. In order to show more clearly the

effect of increasing ψ_{LE} on the maximum lift coefficient, the value of the maximum lift coefficient determined from figure 3 is plotted against ψ_{LE} in figure 4. On the basis of the correlation presented in figure 1, the data of figure 4 indicate that maximum lift coefficients somewhat greater than 1.3 are possible for symmetrical airfoils of 6-percent thickness in the smooth surface condition. The effect of ψ_{LE} on the maximum lift of the airfoils in the rough condition is seen to be less favorable than for the smooth airfoils. The data of figure 4 also indicate that, at least for the particular form of the ψ distribution chosen, increasing the value of ψ_{LE} beyond about 0.20 will probably not result in any further significant increases in maximum lift. Some indication as to the reason for this can be found in figure 5 in which the values of $\Delta v_a/V$, the additional velocity ratio due to angle of attack at a lift coefficient of 1.0, and v/V, the velocity ratio due to the basic thickness form at zero lift, are plotted against ψ_{LE} for the 0-, 0.5-, and 0.75-percent-chord stations. These particular stations were chosen because the peak negative pressure coefficient in the vicinity of maximum lift usually occurs at one or the other. The total velocity ratio at a particular station is obtained from the relation $\left(\frac{v}{V} + \frac{\Delta v_a}{V} c_l\right)$ where c_l is the lift coefficient under consideration. The value of v/V is, of course, zero at the 0-percent-chord station. The value of $\Delta v_a/V$ at the 0-percent-chord station is seen to decrease rapidly with increasing values of ψ_{LE} until values of ψ_{LE} of about 0.2 are reached after which it is seen to decrease relatively slowly with further increases in ψ_{LE}. Both $\Delta v_a/V$ and v/V at the 0.5- and 0.75-percent-chord stations vary rather slowly with increasing ψ_{LE}.

The value of $\Delta v_a/V$ at the leading edge was found to control the predicted value of the maximum lift coefficient until ψ_{LE} reached a value of about 0.166 $\left(A_2 = 1.0\right)$ after which the pressure at the 0.5 station became the controlling factor. Any further variations in maximum lift associated with increasing ψ_{LE} beyond about 0.20 $\left(A_2 = 1.3\right)$ must be relatively small because of the manner in which $\Delta v_a/V$ and v/V vary with ψ_{LE} for ψ_{LE} greater than 0.2.

A somewhat more graphic illustration of the effect of ψ_{LE} on the pressure distribution can be obtained from figure 6 in which the theoretical pressure coefficients for a lift coefficient of 1.3 are plotted

against chordwise position for three of the airfoils derived and for the NACA 64-006 and NACA 0006 airfoil sections. The peak negative pressure of the NACA 64-006 is seen to be of the order of 3.6 times that of the airfoil with ψ_{LE} of 0.244 $(A_2 = 1.6)$.

The theoretical pressure distributions for airfoils having three different values of ψ_{LE} are shown in figure 7 for the zero lift condition. The corresponding pressure distributions for the NACA 64-006 and NACA 0006 sections are also shown in figure 7 for comparison. It is quite apparent from the shapes of the pressure distribution shown in figure 7 that for the higher values of ψ_{LE} extensive regions of laminar flow cannot be expected. In view of the practical difficulty experienced in obtaining the low-drag coefficients corresponding to extensive laminar layers on NACA 6-series airfoil sections on operational aircraft, however, the exclusion of the possibility of obtaining extensive laminar layers on the new airfoils does not seem particularly important. Perhaps the most noteworthy characteristic of the pressure distributions shown in figure 7 is the high values of the peak negative pressure coefficient associated with the large values of ψ_{LE}. Such high values of the negative pressure coefficient mean low values of the critical Mach number. Numerous experimental investigations of NACA 6-series airfoils at relatively high lift coefficients (for example, see reference 7) have shown, however, that the existence of high negative peaks in the low-speed pressure distribution and the accompanying low theoretical critical Mach numbers are not necessarily indicative of correspondingly low force-divergence Mach numbers. Consequently, it was hoped that the high negative peaks in the low-speed pressure distribution of the new airfoils at low lift coefficients did not necessarily mean that poor aerodynamic characteristics would be obtained at high Mach numbers.

Modification of airfoil shapes and designation.- The shapes of the airfoils having values of ψ_{LE} from 0.098 to 0.244 $(A_2$ from 0 to 1.6$)$ are shown in figure 8. The thickness forms shown for the larger values of A_2 are obviously quite impossible from a practical point of view. It was found, however, that the portions of the airfoils from the vicinity of the maximum thickness position to the trailing edge could be varied through a wide range without materially altering the desirable pressure-recovery characteristics at high lift coefficients.

Because of the uncertainty of both the predicted effect of airfoil shape on the maximum lift coefficient and of the effect of the high negative pressures on the airfoils at low lift on the high-speed characteristics, two representative airfoils of the new series were modified

so as to have shapes of practical interest and these airfoils were investigated in the low-turbulence pressure tunnel. One of the airfoils modified had a value of A_2 of 1.3 (ψ_{LE} = 0.20). This particular airfoil was chosen for modification because, as can be seen from figure 4, most of the gains in maximum lift coefficient might be expected with this section and the peak negative pressure coefficient at zero lift for this airfoil is lower than that of the airfoil having A_2 = 1.6. The other airfoil developed for investigation was not a modification of one of those shown in figure 8, but had a value of ψ_{LE} of 0.138 (A_2 = 0.7). This particular section was developed because a rather high maximum lift coefficient would be expected (fig. 4) together with a peak negative pressure coefficient at zero lift substantially lower than that of the airfoil with A_2 = 1.3 (interpolate values in fig. 7).

Because of the experimental nature of the two new sections, a completely systematic and descriptive method of designating the sections does not seem appropriate at present. Hereafter, the new sections are referred to merely as NACA 1-006 and NACA 2-006. The NACA 1-006 has a value of ψ_{LE} of 0.2 (A_2 of 1.3) and the NACA 2-006 has a value of ψ_{LE} of 0.138 (A_2 of 0.7). The 006 has the same meaning as the last three digits in the designation of NACA 6-series airfoils; that is, in the present case, the 006 means the airfoils are symmetrical and are of 6-percent thickness. Sketches of the NACA 1-006 and NACA 2-006 are shown in figure 9 in comparison with the NACA 64-006 and NACA 0006. The predicted maximum lift coefficients of the two sections are 1.32 and 1.22 for the NACA 1-006 and NACA 2-006, respectively, in the smooth surface condition. Ordinates and theoretical low-speed pressure-distribution data are given in tables I and II for the NACA 1-006 and NACA 2-006 airfoil sections. The pressure distribution data are given in the form of the velocity ratio distribution associated with the basic thickness form at zero lift v/V and of the incremental velocity ratio distribution associated with angle of attack $\Delta v_a/V$. The values of $\Delta v_a/V$ are for a lift coefficient of 1.0. The method of combining the velocity ratios v/V and $\Delta v_a/V$ to give the velocity distribution about the airfoil at any lift coefficient is given in reference 1.

APPARATUS, TESTS, AND METHODS

Wind tunnel.- All the tests of the present investigation were made in the Langley low-turbulence pressure tunnel. This tunnel was originally

designed and has been operated for a number of years as a low-speed, high Reynolds number facility. At the present time, the Langley low-turbulence pressure tunnel is also operated as a high-speed research facility with Freon-12 gas replacing air as the test medium. Because the speed of sound in Freon is only about one half of that in air, choking Mach numbers can be obtained in the 3- by $7\frac{1}{2}$-foot test section with the original 2000-horsepower drive motor. The variation of the Reynolds number per foot obtainable at three tunnel pressures is shown in figure 10 as a function of Mach number.

In the present investigation, both high and low Mach number tests were made. For the low-speed investigation, the tunnel was filled with air compressed to pressures of as high as 150 pounds per square inch. The desired Reynolds number dictated the value of the tunnel pressure. The high Mach number investigation was made in Freon-12 at a tunnel pressure of 16 inches of mercury absolute and with a Freon purity of approximately 95 percent by weight.

Models and test methods.- The NACA 1-006 and NACA 2-006 sections were investigated at both high and low Mach numbers and the NACA 64-006 section was investigated at high Mach numbers for purposes of comparison. The models of the NACA 64-006 and the NACA 1-006 were machined from solid steel and the model of the NACA 2-006 was machined from solid dural. The three models were of 1-foot chord. The models when mounted in the tunnel completely spanned the 3-foot dimension so that two-dimensional flow was obtained. Each end of the model passed through a slot in the tunnel wall. One end of the model was attached to the two-dimensional-tunnel semispan balance in such a way that no constraint was applied in yaw and roll. The lift and drag forces were restrained at the other end of the model which was pivoted in a universal bearing. With this system of mounting, the semispan balance measured one-half the lift and drag forces and all of the pitching moment. A labyrinth-type seal was provided at each end of the model to minimize the effect of air leakage through the slots in the tunnel wall. The effectiveness of the seal is indicated by the fact that the drag as measured by the balance was found to be unaffected by variations in the pressure difference between the inside and outside of the tunnel test section. A sketch showing the relationship between the ends of the model, the tunnel wall, the labyrinth seal, the mounting pivot, and balance is presented in figure 11. A photograph of the NACA 2-006 airfoil section mounted in the tunnel is shown in figure 12.

The semispan balance was employed for making lift, drag, and pitching-moment measurements in the high Mach number tests and for the lift and pitching-moment measurements in the low-speed tests. Drag measurements were made in the low-speed tests by the wake-survey method. In order to check the accuracy of the drag data obtained at high Mach

numbers with the semispan balance, comparative values of the drag were determined from point-by-point measurements of the static pressure and total pressure defect in the wake for the NACA 1-006 airfoil and the NACA 64-006 airfoil at several angles of attack. The wake-survey measurements were not made simultaneously with the balance measurements and were obtained at only one spanwise station. Since the balance integrates the drag across the entire span and because of the difficulty of determining the exact width of the wake at high Mach numbers, some differences in the drag coefficients as determined by the two techniques might be expected. The drag data obtained by the two methods, shown in figure 13 as a function of Mach number, do indicate some differences, however, these differences are small in most cases and do not appear to form any consistent trend. It was concluded, therefore, that the drag measurements made with the balance were as good if not better than those determined by the wake-survey method. Some comparisons at low speeds of lift coefficients as determined by integration of the pressure reaction upon the floor and ceiling of the tunnel and by the semispan balance showed excellent agreement.

Tests.- The low-speed investigation consisted in measurements of the lift, drag, and pitching moment of the NACA 1-006 and NACA 2-006 airfoil sections at different Reynolds numbers and for the smooth and rough surface conditions. The leading-edge roughness employed was the same as that used in previous two-dimensional investigations and consisted in 0.011-diameter carborundum grains thinly spread over a surface length of 8-percent chord back from the leading edge. The Mach number of the low-speed tests did not exceed 0.15. Lift, drag, and pitching-moment data were obtained for the NACA 1-006 in both the smooth and rough surface conditions at Reynolds numbers of 3.0×10^6, 6.0×10^6, and 9.0×10^6. Lift and drag data were obtained for the NACA 2-006 at the same three Reynolds numbers in the smooth condition and pitching-moment data were obtained at 3.0×10^6 and 9.0×10^6. Lift, drag, and pitching-moment data were obtained for the NACA 2-006 airfoil section in the rough surface condition only at a Reynolds number of 6.0×10^6.

In the high-speed investigation, data were obtained only for the smooth surface condition. The lift, drag, and pitching-moment characteristics of the NACA 1-006, NACA 2-006, and NACA 64-006 were determined for a Mach number range extending from 0.3 or 0.4 to a Mach number which was limited by model vibration. The angle-of-attack range of the tests extended from 0° to 6°. The variation of Reynolds number with Mach number for a tunnel pressure of 16 inches of mercury and Freon purity of 95 percent is shown in figure 10.

CORRECTIONS

Wind-tunnel-wall corrections.- The low and high Mach number data have been corrected for tunnel-wall effects according to the methods of references 1 and 8. The magnitude of the corrections were very small in all cases. The maximum correction occurred at the highest Mach numbers and was of the order of 2 to 3 percent. The very small angle-of-attack correction indicated in reference 8 was not applied.

Freon corrections.- Corrections must be applied in order to convert data obtained in Freon to equivalent air data. These corrections have been fully discussed in reference 9 and have been applied to all the high-speed data of the present investigation. The magnitude of the corrections is rather small. For example, the measured Freon Mach number differs by as much as 3.0 percent from its equivalent air Mach number and the measured lift and moment coefficients differ by as much as 4 to 8 percent from their equivalent values in air. The corresponding drag-coefficient correction is of the order of 2 to 5 percent.

RESULTS AND DISCUSSION

The discussion will deal first with the low-speed results obtained for the different airfoils after which the high-speed data will be considered.

Low-Speed Characteristics

The low-speed data obtained for the NACA 1-006 and NACA 2-006 airfoil sections are presented in standard coefficient form in figures 14 and 15. The lift and quarter-chord pitching-moment data are given in figures 14(a) and 15(a), and the drag data together with the pitching-moment data referred to the aerodynamic center are given in figures 14(b) and 15(b).

Lift.- An examination of the lift data of figures 14(a) and 15(a) indicates that maximum lift coefficients of about 1.3 were obtained for both airfoils in the smooth surface condition at a Reynolds number of 9.0×10^6. The data of figure 15(a) indicate that the nose of the NACA 2-006 model was slightly unsymmetrical as evidenced by maximum lift coefficients of 1.26 and 1.32 on the positive and negative side of the lift curve, respectively. Reductions in the Reynolds number from 9.0×10^6 to 3.0×10^6 are seen to cause a decrease of about 0.1 in the maximum lift coefficient of both airfoils with most of the scale

effect occurring between 9.0×10^6 and 6.0×10^6. A comparison of the lift curves obtained for the NACA 1-006 and NACA 2-006 airfoil sections with that for the NACA 64-006 airfoil section (taken from reference 1) is shown in figure 16 for a Reynolds number of 9.0×10^6. The two new sections are seen to have maximum lift coefficients which are of the order of 63 percent higher than the value of 0.8 obtained for the NACA 64-006 section. It is perhaps of some interest to point out that the values of the maximum lift coefficient obtained for the NACA 1-006 and the NACA 2-006 are of the same order as the values of 1.32 and 1.22 predicted by the method described in a previous section of the paper.

The addition of standard leading-edge roughness is seen to reduce the values of the maximum lift coefficient of the NACA 1-006 and NACA 2-006 airfoils to about 0.8, which value is characteristic of other symmetrical airfoils of 6-percent thickness in the smooth and rough surface condition. Thus, maximum lift coefficients of the order of 1.3 can be expected from the new airfoils only if the leading edges are smooth. This result indicates the importance of surface condition; however, the construction and maintenance of a wing sufficiently smooth to permit the attainment of the high maximum lift coefficients is believed to be less difficult than the construction and maintenance of a 6-series low-drag wing in a sufficiently smooth and fair condition to permit the attainment of extensive laminar flows because it would probably be necessary to maintain only the first 3 or 4 percent of the wing smooth in order to obtain the high maximum lift coefficients.

Further examination of the data of figures 14(a) and 15(a) indicates that the character of the stall of both new airfoils is relatively gradual at all three Reynolds numbers with the exception of that for the NACA 2-006 at a Reynolds number of 3.0×10^6. There appears to be no appreciable difference in the lift-curve slopes of the NACA 1-006 and NACA 2-006 airfoil sections for Reynolds numbers of 3.0×10^6 and 6.0×10^6 (figs. 14(a) and 15(a)). The lift-curve slope of the the NACA 2-006, however, is higher than that of the NACA 1-006 for a Reynolds number of 9.0×10^6. The results shown in figure 16 indicate that at a Reynolds number of 9.0×10^6 the lift-curve slope of the NACA 64-006 is about the same as that of the NACA 1-006 but is less than that of the NACA 2-006.

Pitching moment.- The pitching-moment data of figures 14 and 15 do not appear to warrant any particular comment as they are not unusual in any respect.

Drag.- As would be expected, the data of figures 14(b) and 15(b) show that the drag coefficients of the NACA 1-006 and 2-006 airfoil

sections are relatively high in the low lift-coefficient range. Perhaps the most unusual characteristic of the drag polars for the two new airfoils is the manner in which the drag of the smooth sections decreases as the lift coefficient is increased from 0 to about 0.5, thus the minimum drag occurs at a lift coefficient of about 0.5 rather than at zero lift. This rather peculiar behavior of the drag polars of the two new sections in the smooth condition may possibly be attributed to the fact that as the lift coefficient is varied from zero, the pressure gradient on one surface becomes less adverse and the relative extent of laminar flow on this surface increases. With the exception of a somewhat higher drag at zero lift for the NACA 1-006, there do not appear to be any very important differences in the drag characteristics of the two airfoil sections. Increases in the Reynolds number are seen to have some favorable effect on the drag coefficient at most lift coefficients. The addition of leading-edge roughness increases the drag coefficient at all lift coefficients for both airfoil sections. The asymmetry of the drag polars in the rough surface condition probably results from a difference in the amount of roughness on the upper and lower surfaces.

A comparison of the drag polars of the NACA 1-006 and NACA 2-006 airfoil sections with that of the NACA 64-006 (reference 1) is shown in figure 17 for the smooth surface condition and a Reynolds number of 9.0×10^6. The minimum drag coefficients of the new sections are seen to be about 0.0020 higher than that of the NACA 64-006 and, of course, occur at a lift coefficient of about 0.5 rather than at zero lift. It should be remembered that the very low drag coefficients of the NACA 64-006 can only be obtained if extensive laminar layers are obtained and that the maintenance of large portions of practical airplane wings in a sufficiently fair and smooth condition to insure the attainment of extensive laminar layers has met with no great amount of success in the past. It may also be of some interest to note that the maximum section lift to drag ratios for the new sections are about the same as that for the NACA 64-006.

The drag polars corresponding to the rough surface condition for the two new sections and the NACA 64-006 (reference 1) show no important differences.

High-Speed Characteristics

The lift, pitching moment, and drag are plotted against Mach number for the three airfoil sections and for various angles of attack in figures 18 to 20. In those cases for which the choking Mach number was approached, the curves are dotted beginning at a Mach number of 0.03 less than that for choke. The lift coefficient is plotted against angle of attack in figure 21 for different Mach numbers and the pitching moment

and drag are plotted against lift coefficient for different Mach numbers in figures 22 and 23. These curves were obtained by cross plotting the data of figures 18 to 20. Unfortunately, the high-speed results are rather incomplete because of the limited range of angle of attack for which data could be obtained.

Lift.- The lift data for all three airfoils are plotted together in figure 18. The data of figure 18 indicate that no very consistent or important differences exist in the lift characteristics of the NACA 1-006, NACA 2-006, and NACA 64-006 airfoil sections, at least at 0°, 2°, and 4° angle of attack. The lift coefficients of the NACA 64-006 airfoil section, however, appear to be higher than those of the NACA 2-006 section for Mach numbers greater than 0.6 at an angle of attack of 6°. These trends are also evident in the plot of lift against angle of attack shown for the three airfoils and different Mach numbers in figure 21. The data of figure 21 seem to indicate that the maximum lift coefficients of the new sections at high Mach numbers may be lower than that of the NACA 64-006; however, the results are not sufficiently complete to establish this fact with certainty.

Pitching moment.- The quarter-chord pitching-moment characteristics of the three airfoil sections are plotted against Mach number for different angles of attack in figure 19. These data show practically no differences in the pitching-moment characteristics of the three airfoil sections. The same conclusion is evident in the curves of pitching moment against lift coefficient shown in figure 22.

Drag.- The drag characteristics of the three airfoils which are shown in three parts in order to avoid confusion (figs. 20(a), 20(b), and 20(c)) indicate that the Mach number corresponding to drag divergence is considerably lower for the NACA 1-006 than for the NACA 64-006 at all angles of attack although the drag rise with Mach number seems to be less steep for the new section in most cases. The NACA 2-006 is seen to represent quite an improvement over the NACA 1-006 in that drag divergence occurs at higher Mach numbers. In fact, at an angle of attack of 0°, there seems to be relatively little difference in the drag characteristics of the NACA 2-006 and the NACA 64-006 airfoil sections (figs. 20(b) and 20(c)). At higher angles of attack, the drag-divergence Mach number of the NACA 2-006 is appreciably lower than that of the NACA 64-006.

Some further insight into the differences in the lift and drag characteristics of the new airfoils and the NACA 64-006 airfoil at high Mach numbers can be found in figure 23 in which drag coefficient has been plotted against lift coefficient for the three airfoils at different Mach numbers. It is evident in the data of figure 23 that the drag of the NACA 64-006 airfoil is substantially lower than that of either of the new airfoils for Mach numbers above 0.65 and for lift coefficients

above about 0.1. It is also clear that the drag characteristics of the NACA 2-006, although not as good as those of the NACA 64-006, are much better than those of the NACA 1-006.

The fact that the high-speed drag characteristics of the NACA 2-006 are much better than those of the NACA 1-006 seems particularly significant in view of the fact that the maximum lift coefficient of the NACA 2-006 at low speeds is not substantially different from that of the NACA 1-006. This result might be interpreted as indicating that additional airfoils can be designed which have somewhat sharper leading edges than the NACA 2-006 without causing significant reductions in the maximum lift coefficient but which will have high-speed drag characteristics better than those of the NACA 2-006 and more nearly approaching those of the NACA 64-006.

CONCLUDING REMARKS

An investigation has been made to determine whether thin airfoils can be developed which have increased values of the low-speed maximum lift coefficient but which at the same time retain the basic advantages of thin sections at high Mach numbers. Airfoil data which are available in the literature were analyzed and an approximate relation between the airfoil pressure distribution and the maximum lift coefficient was found. With the use of this relation as a guide, several thin airfoil sections were derived. Two of these experimental airfoil sections which were symmetrical and 6 percent thick were investigated at both high and low subsonic Mach numbers. The following important results were obtained from the investigation:

1. Both of the new airfoil sections had low-speed maximum lift coefficients in the smooth surface condition of about 1.3 at a Reynolds number of 9.0×10^6 as compared to values of about 0.8 which are characteristic of other 6-percent-thick symmetrical airfoil sections. The maximum lift coefficients of the new sections with roughened leading edges were no higher than those of other symmetrical airfoils of 6-percent thickness with leading-edge roughness.

2. No significant differences were found in the lift and moment characteristics of the new sections as compared to the NACA 64-006 section at high Mach numbers at least through most of the limited angle-of-attack range of the present investigation (maximum angle of attack for the high-speed tests was 6°).

3. The drag divergence Mach numbers of the new sections were lower than those of the NACA 64-006. The data for the two new sections,

however, indicate the possibility that other airfoils, which have increased values of the drag divergence Mach number with but little decrease in the low-speed maximum lift coefficient, can be designed.

Langley Aeronautical Laboratory
National Advisory Committee for Aeronautics
Langley Field, Va.

REFERENCES

1. Abbott, Ira H., Von Doenhoff, Albert E., and Stivers, Louis S., Jr.: Summary of Airfoil Data. NACA Rep. 824, 1945. (Formerly NACA ACR L5C05.)

2. Loftin, Laurence K., Jr., and Bursnall, William J.: The Effects of Variations in the Reynolds Number between 3.0×10^6 and 25.0×10^6 upon the Aerodynamic Characteristics of a Number of NACA 6-Series Airfoil Sections. NACA Rep. 964, 1950. (Formerly NACA TN 1773.)

3. Jacobs, Eastman N., and Sherman, Albert: Airfoil Section Characteristics as Affected by Variations of the Reynolds Number. NACA Rep. 586, 1937.

4. Von Doenhoff, Albert E., and Tetervin, Neal: Determination of General Relations for the Behavior of Turbulent Boundary Layers. NACA Rep. 772, 1943. (Formerly NACA ACR 3G13.)

5. McCullough, George B., and Gault, Donald E.: Boundary-Layer and Stalling Characteristics of the NACA 64A006 Airfoil Section. NACA TN 1923, 1949.

6. Theodorsen, T., and Garrick, I. E.: General Potential Theory of Arbitrary Wing Sections. NACA Rep. 452, 1933.

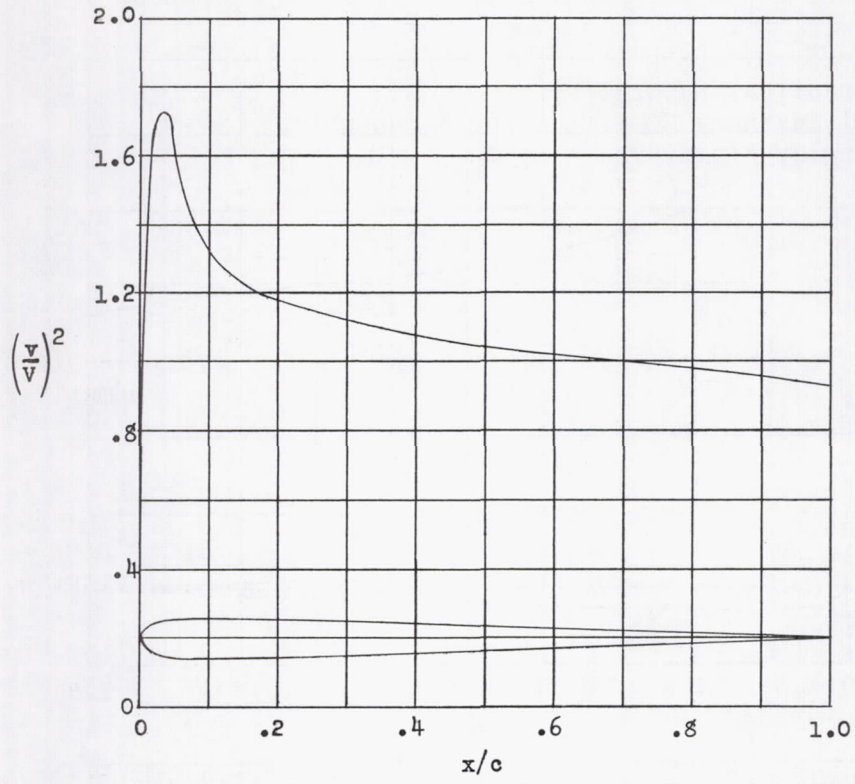
7. Van Dyke, Milton D., and Wibbert, Gordon A.: High-Speed Aerodynamic Characteristics of 12 Thin NACA 6-Series Airfoils. NACA MR A5F27, Army Air Forces, 1945.

8. Allen, H. Julian, and Vincenti, Walter G.: Wall Interference in a Two-Dimensional-Flow Wind Tunnel, with Consideration of the Effect of Compressibility. NACA Rep. 782, 1944.

9. Von Doenhoff, Albert E., and Braslow, Albert L.: Studies of the Use of Freon-12 as a Testing Medium in the Langley Low-Turbulence Pressure Tunnel. NACA RM L51I11, 1951.

TABLE I

ORDINATES AND PRESSURE-DISTRIBUTION DATA FOR THE NACA 1-006 AIRFOIL SECTION



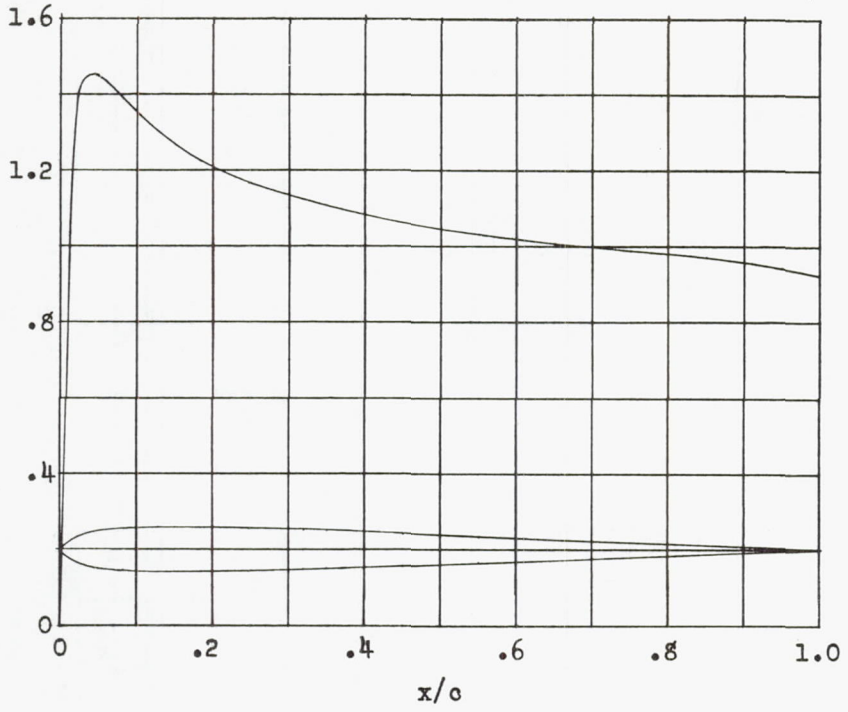
x (percent c)	y (percent c)	$(v/V)^2$	v/V	$\Delta v_a/V$
0	0	0	0	2.070
.434	1.154	.846	.920	1.749
1.769	2.123	1.677	1.295	1.223
4.081	2.752	1.698	1.303	.813
7.522	2.987	1.416	1.190	.548
12.174	2.990	1.266	1.125	.407
17.868	2.917	1.195	1.093	.319
24.376	2.757	1.153	1.074	.262
31.538	2.524	1.113	1.055	.217
35.00	2.396	1.098	1.048	.200
40.00	2.212	1.075	1.037	.179
45.00	2.028	1.059	1.029	.161
50.00	1.844	1.040	1.020	.145
55.00	1.659	1.028	1.014	.130
60.00	1.475	1.020	1.010	.117
65.00	1.291	1.008	1.004	.105
70.00	1.106	1.000	1.000	.095
75.00	.922	.988	.994	.083
80.00	.737	.980	.990	.070
85.00	.553	.970	.985	.060
90.00	.369	.958	.979	.046
95.00	.184	.943	.971	.031
100.00	0			0

L. E. radius: 1.575 percent c

NACA

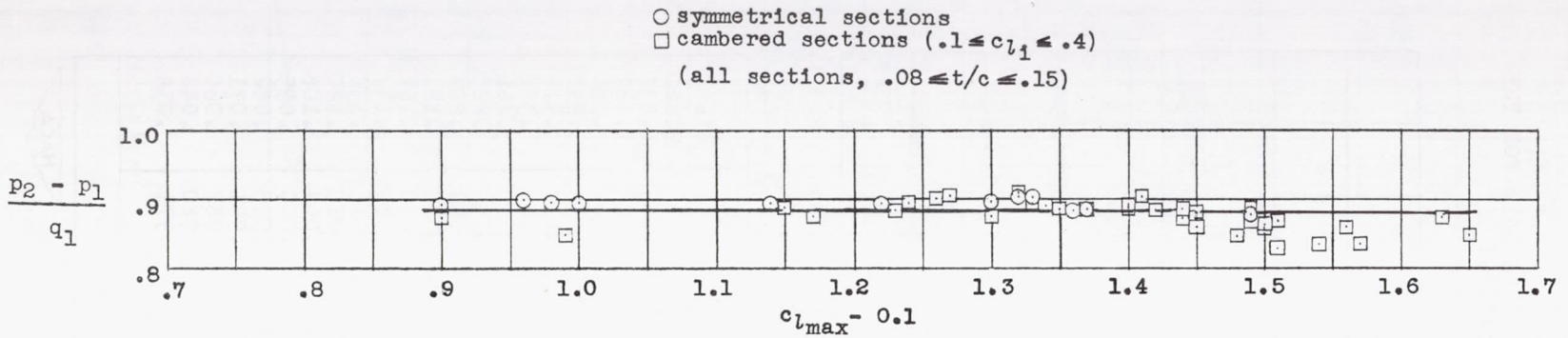
TABLE II

ORDINATES AND PRESSURE-DISTRIBUTION DATA FOR THE NACA 2-006 AIRFOIL SECTION

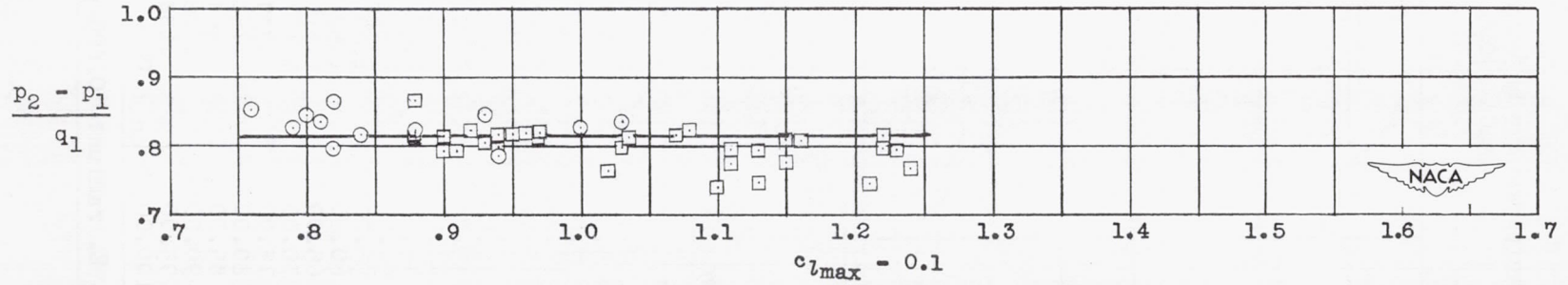


x (percent c)	y (percent c)	$(v/V)^2$	v/V	$\Delta v_a/V$
0	0	0	0	2.600
.501	.937	.914	.956	1.833
2.008	1.769	1.397	1.182	1.127
4.541	2.413	1.457	1.207	.760
8.114	2.818	1.390	1.179	.548
12.717	2.983	1.304	1.142	.416
18.292	2.962	1.225	1.107	.328
24.727	2.810	1.166	1.080	.266
31.828	2.561	1.121	1.059	.220
35.00	2.442	1.105	1.051	.203
40.00	2.254	1.082	1.040	.181
45.00	2.066	1.061	1.030	.162
50.00	1.878	1.047	1.023	.147
55.00	1.691	1.032	1.016	.132
60.00	1.503	1.020	1.010	.120
65.00	1.315	1.008	1.004	.108
70.00	1.127	1.000	1.000	.095
75.00	.939	.990	.995	.082
80.00	.751	.981	.991	.071
85.00	.564	.974	.987	.060
90.00	.376	.960	.980	.048
95.00	.188	.943	.971	.034
100.00	0			0
L. E. radius: 0.805 percent c				

NACA



(a) Airfoils with smooth surfaces.



(b) Airfoils with standard leading-edge roughness.

Figure 1.- Correlation of pressure-recovery parameter and $\left(c_{l_{max}} - 0.1\right)$.

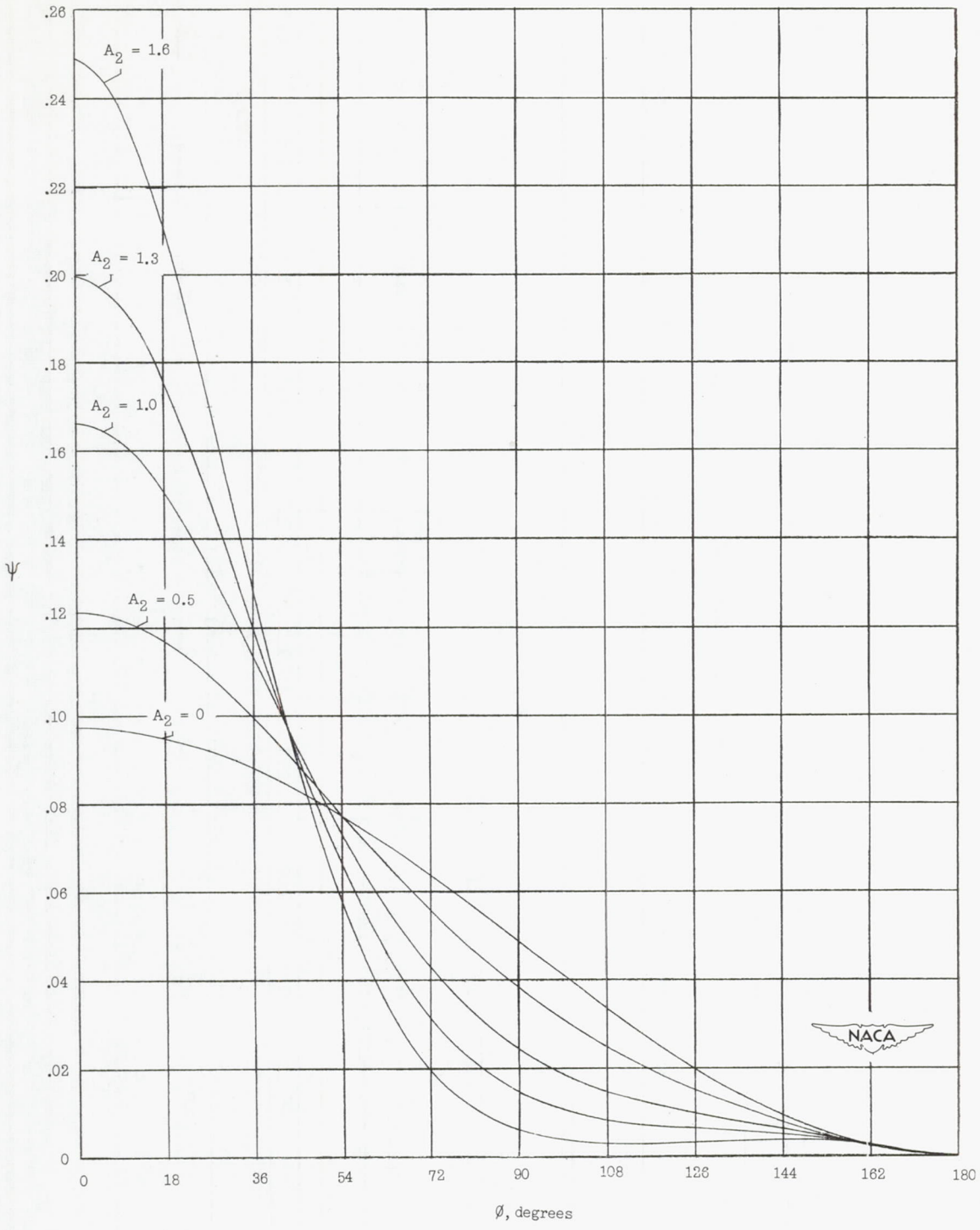


Figure 2.- ψ as a function of ϕ for airfoils having different values of A_2.

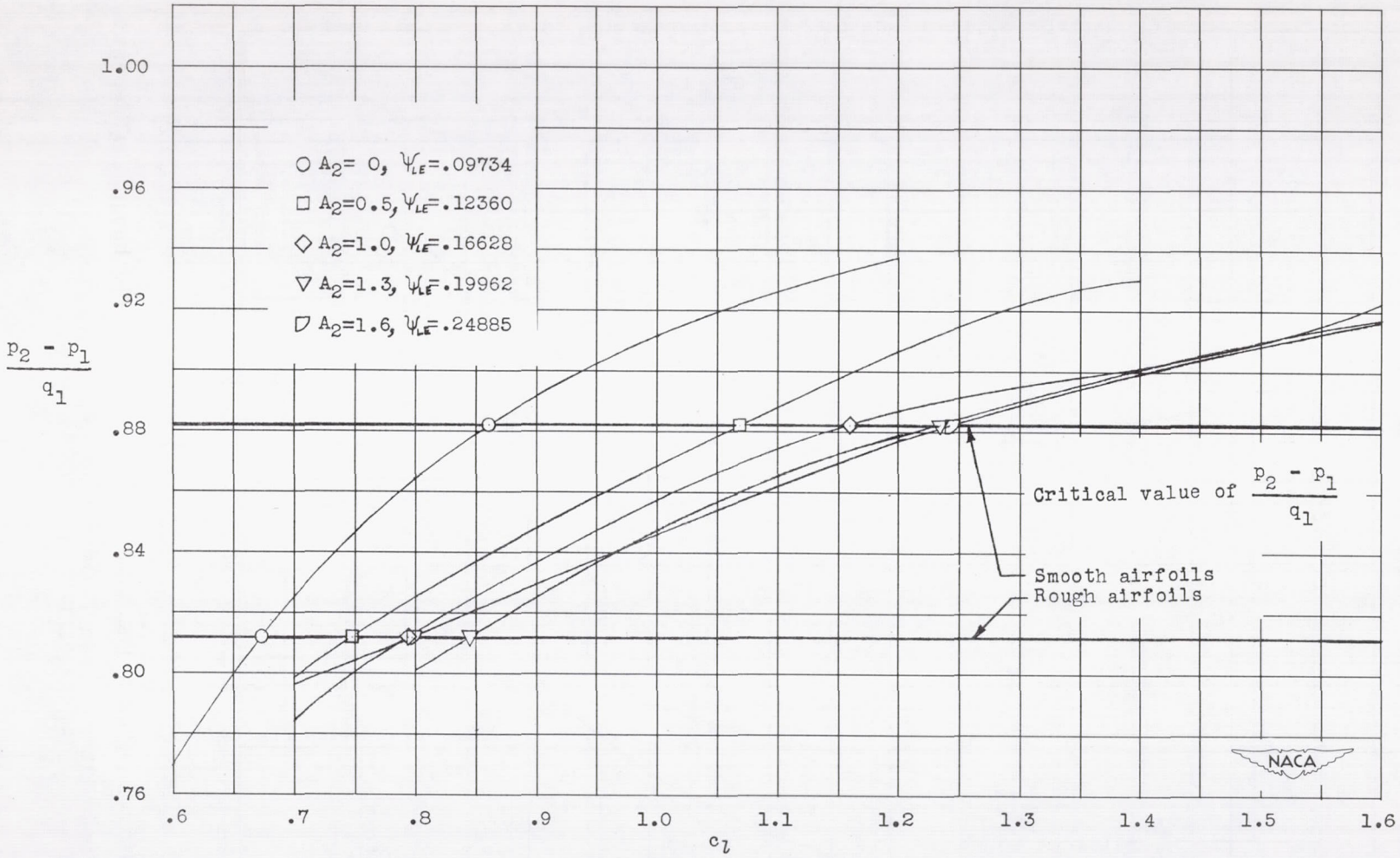


Figure 3.- Pressure-recovery parameter as a function of lift coefficient for several airfoil sections having different values of the parameter A_2.

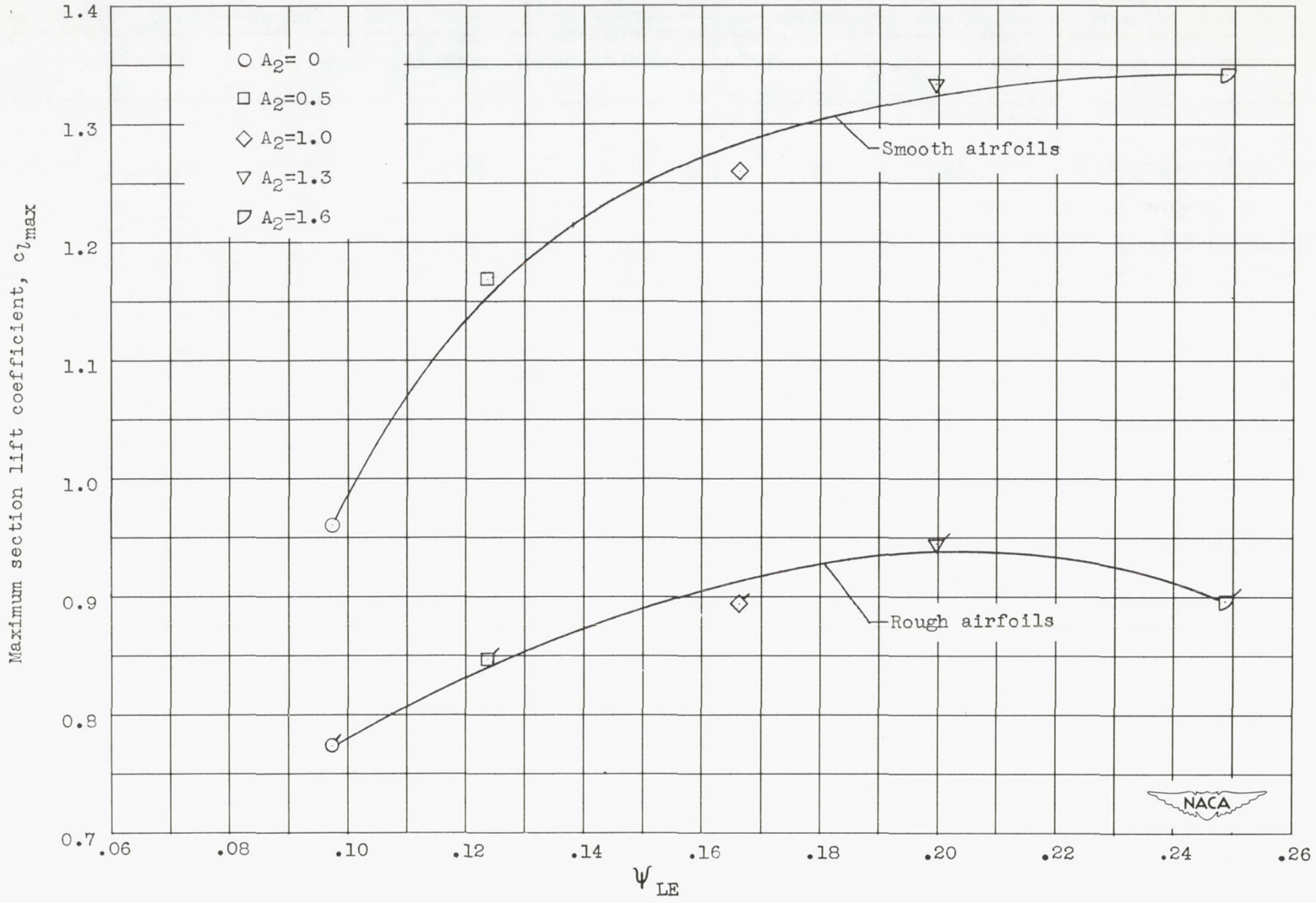


Figure 4.- Effect of the value of ψ at the leading edge on the predicted value of the maximum lift coefficient.

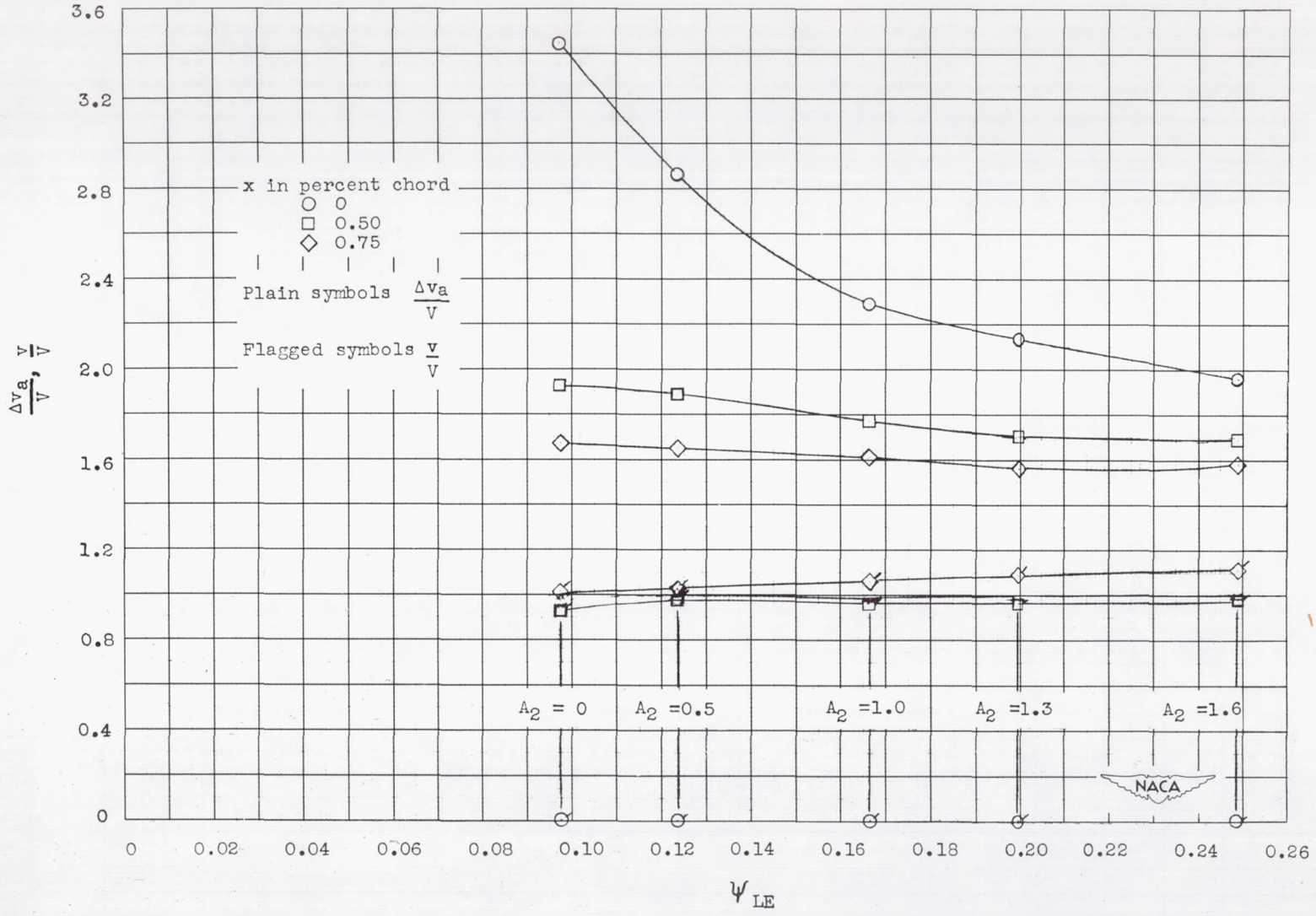


Figure 5.- Effect of ψ at the leading edge on the value of the velocity ratios at several chordwise positions.

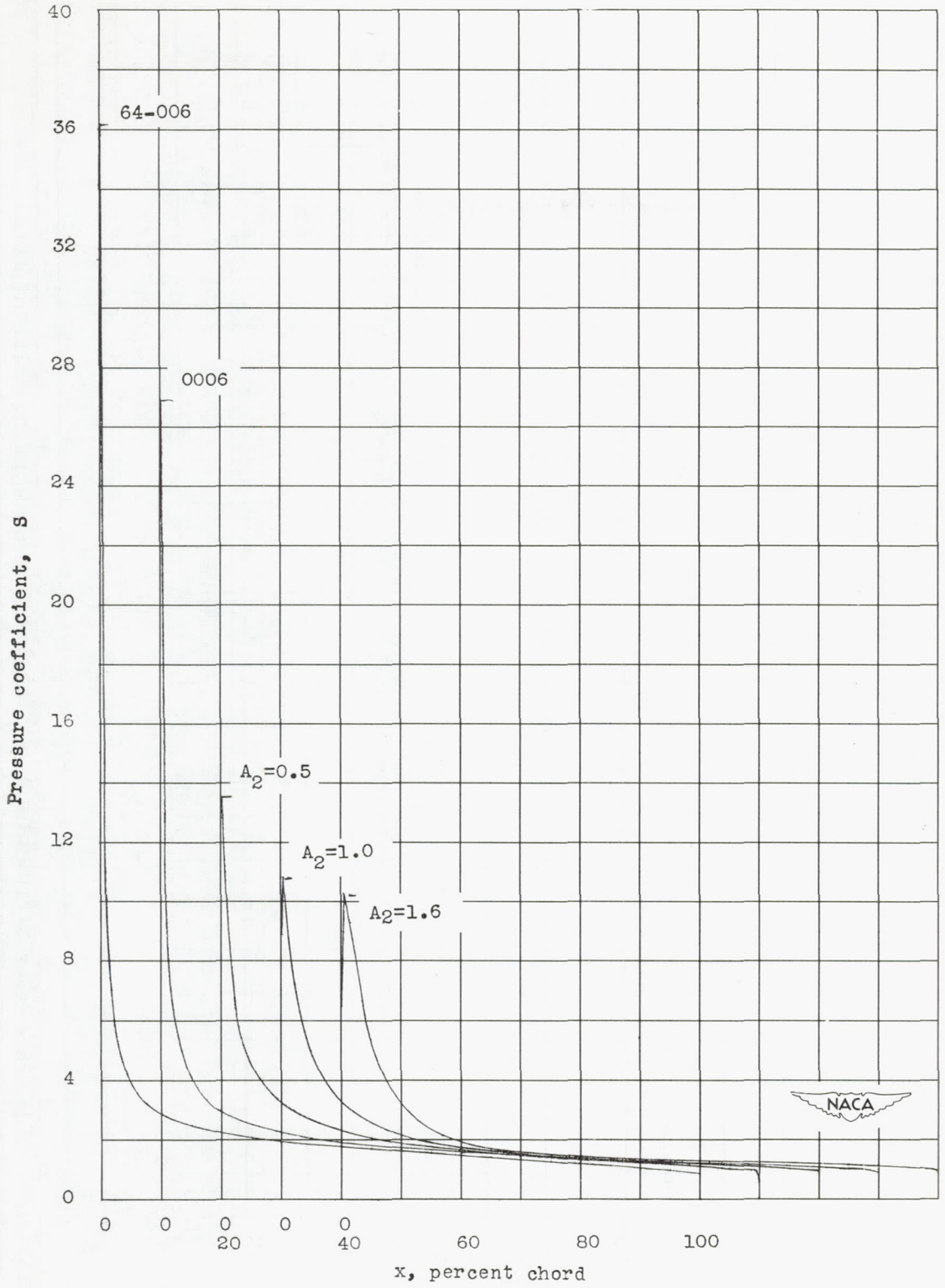


Figure 6.- Comparison of theoretical pressure distribution at a lift coefficient of 1.3 for several airfoil sections.

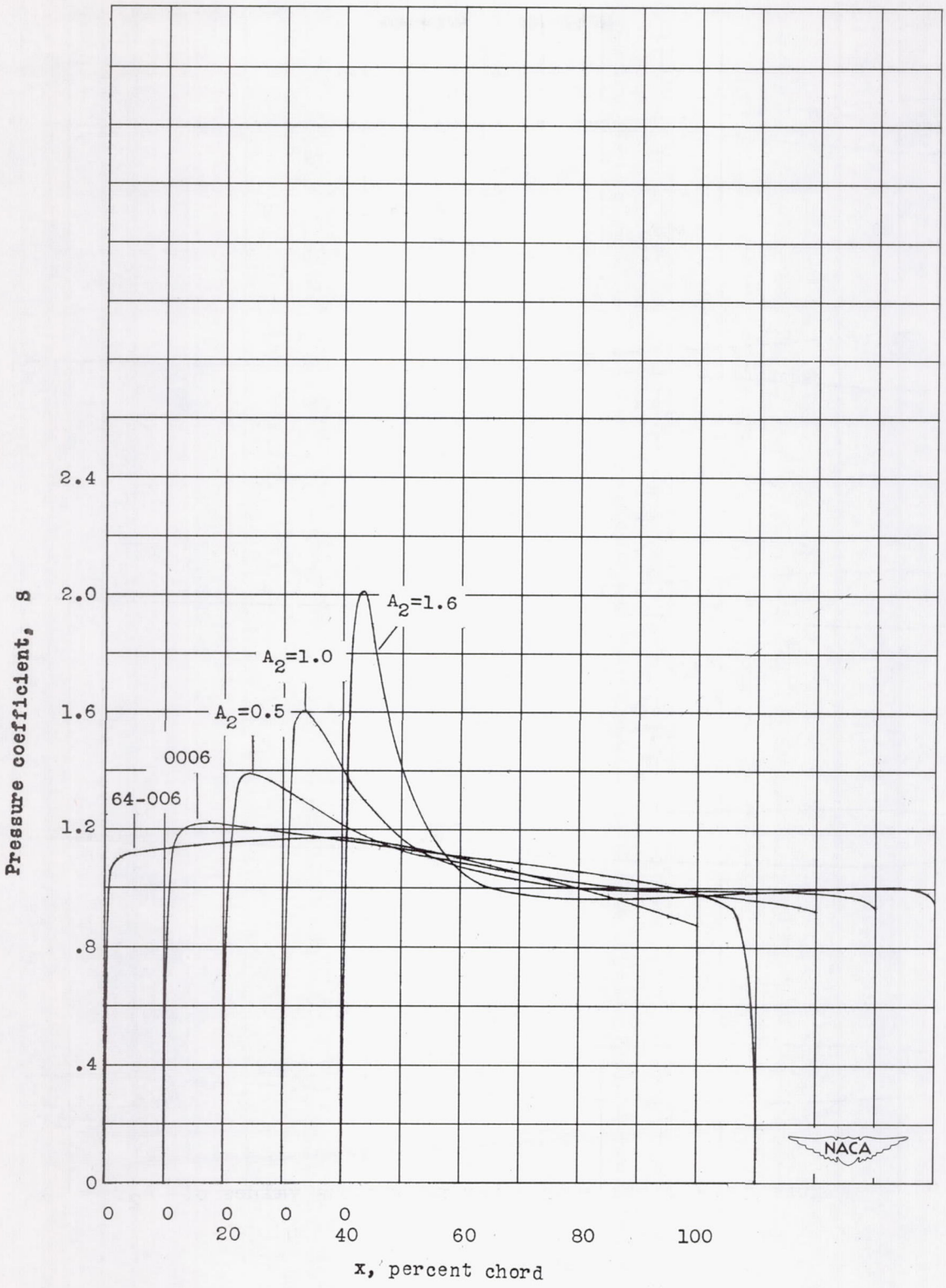


Figure 7.- Comparison of theoretical pressure distribution for several airfoil sections at zero lift.

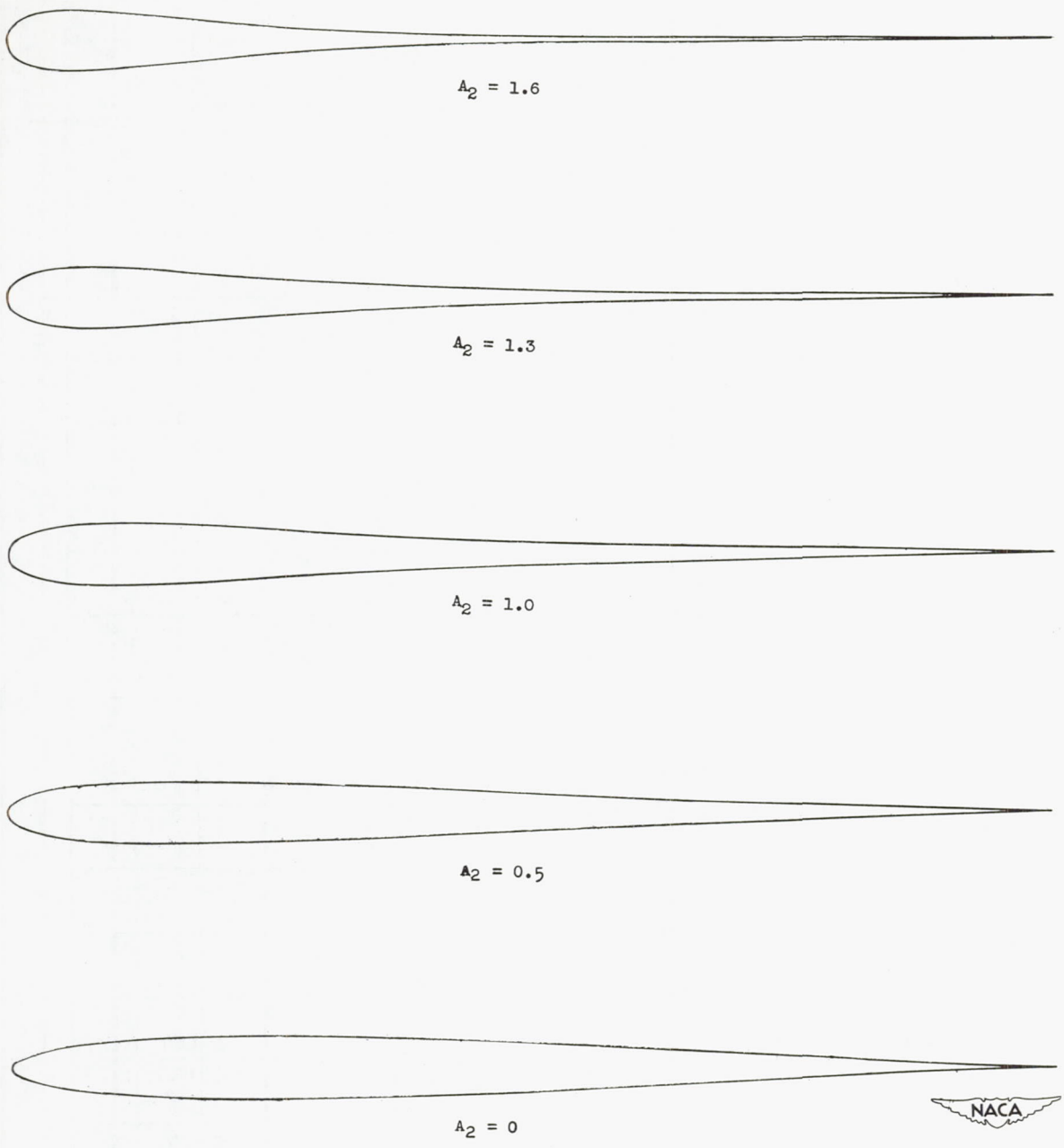


Figure 8.- Airfoil shapes having various values of A_2.

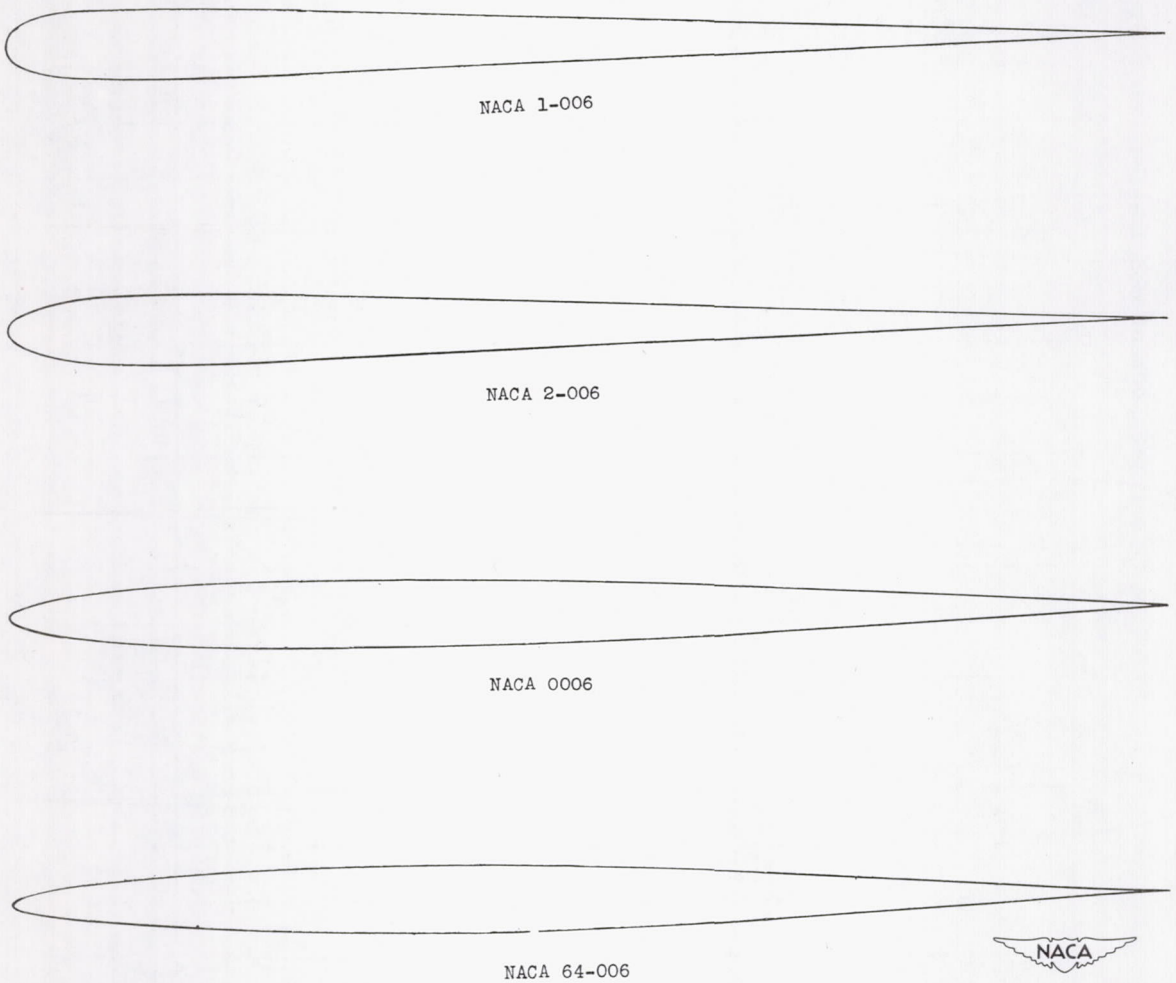


Figure 9.- Comparison of shapes of NACA 1-006 and NACA 2-006 airfoil sections with the NACA 64-006 and NACA 0006 airfoil sections.

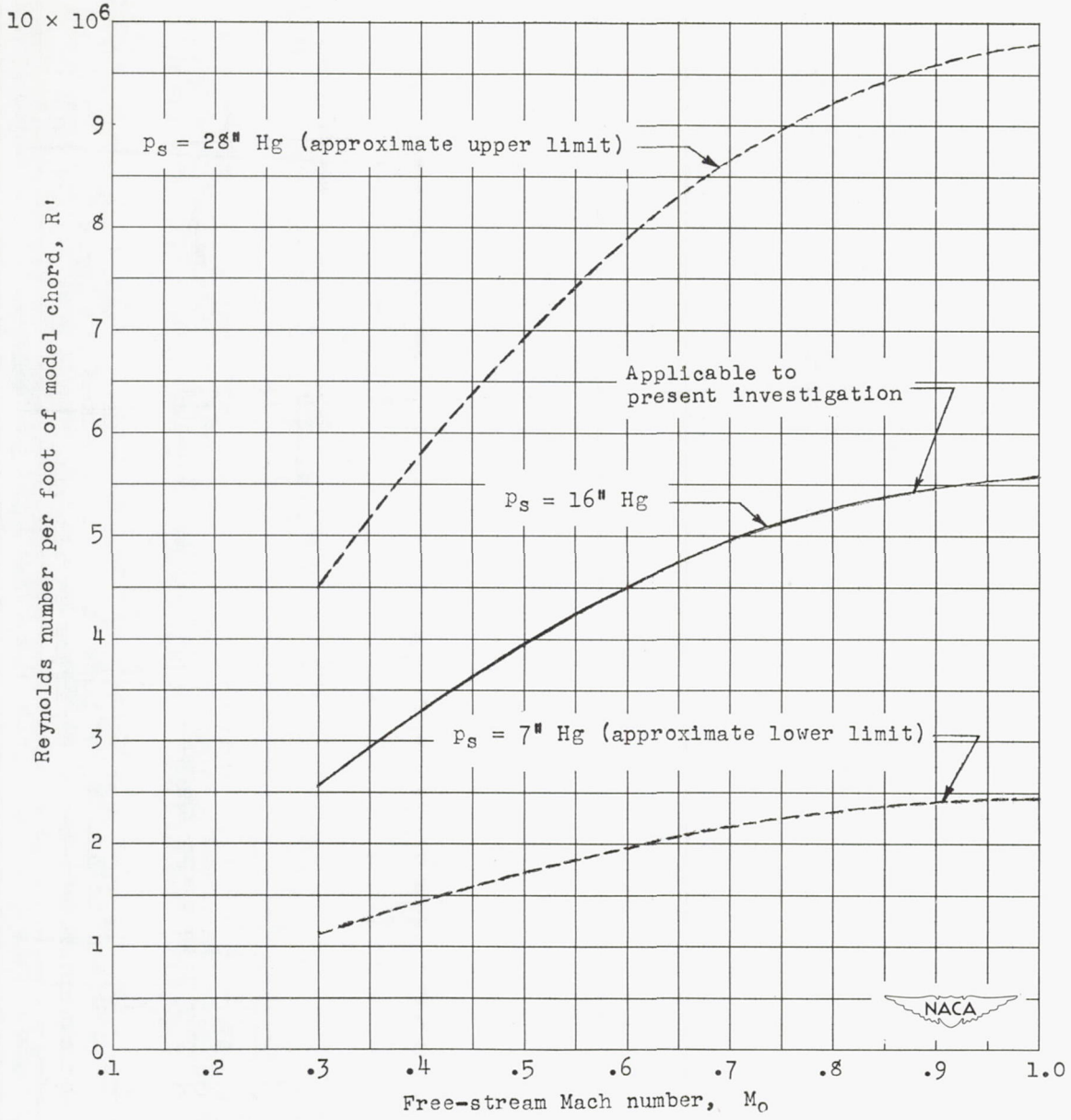


Figure 10.- Variation of Reynolds number with Mach number for a stream mixture of 95 percent Freon and 5 percent air by weight at a stagnation temperature of 80° F.

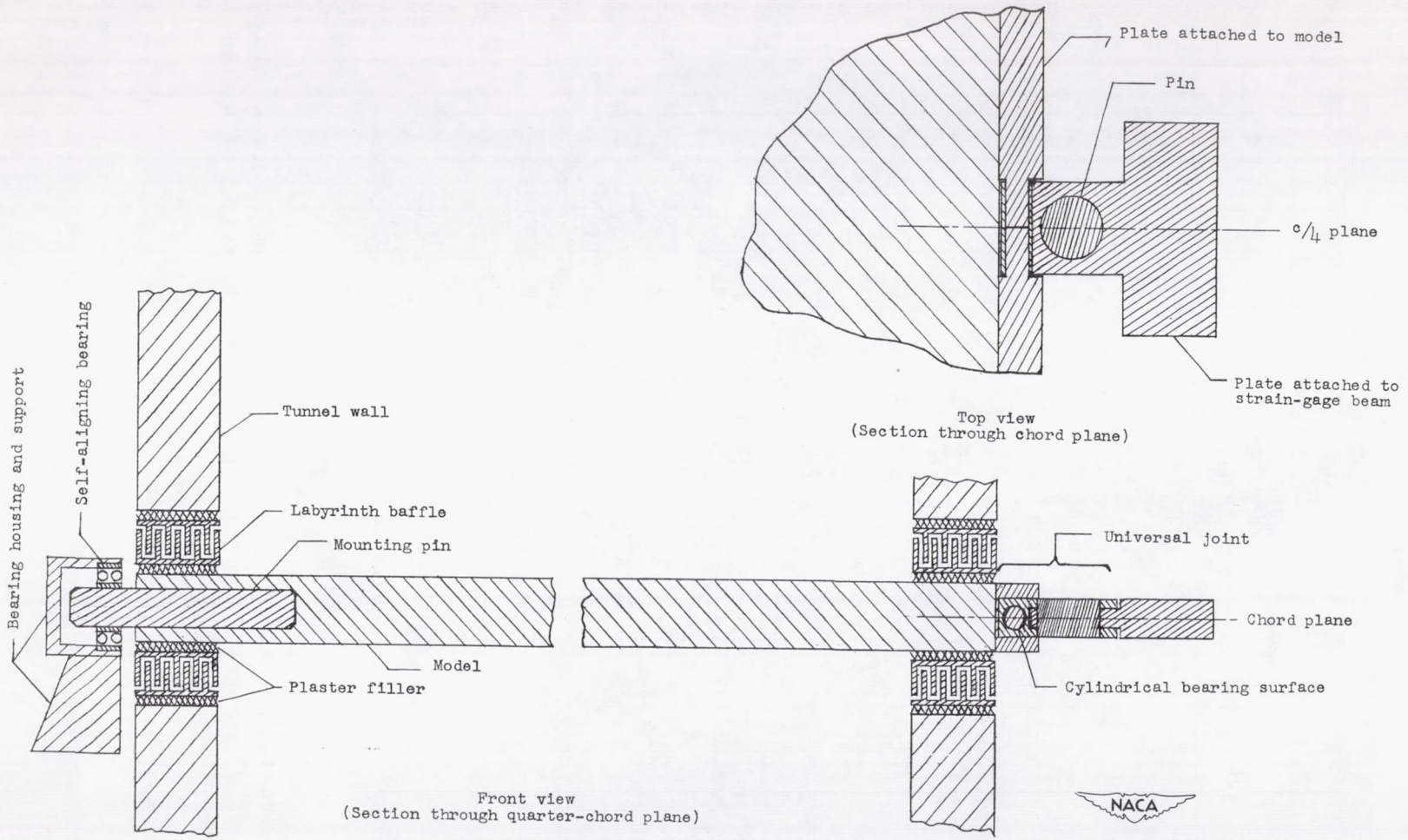


Figure 11.- Schematic drawing of model mounted in tunnel for force and moment measurements employing strain-gage balance.

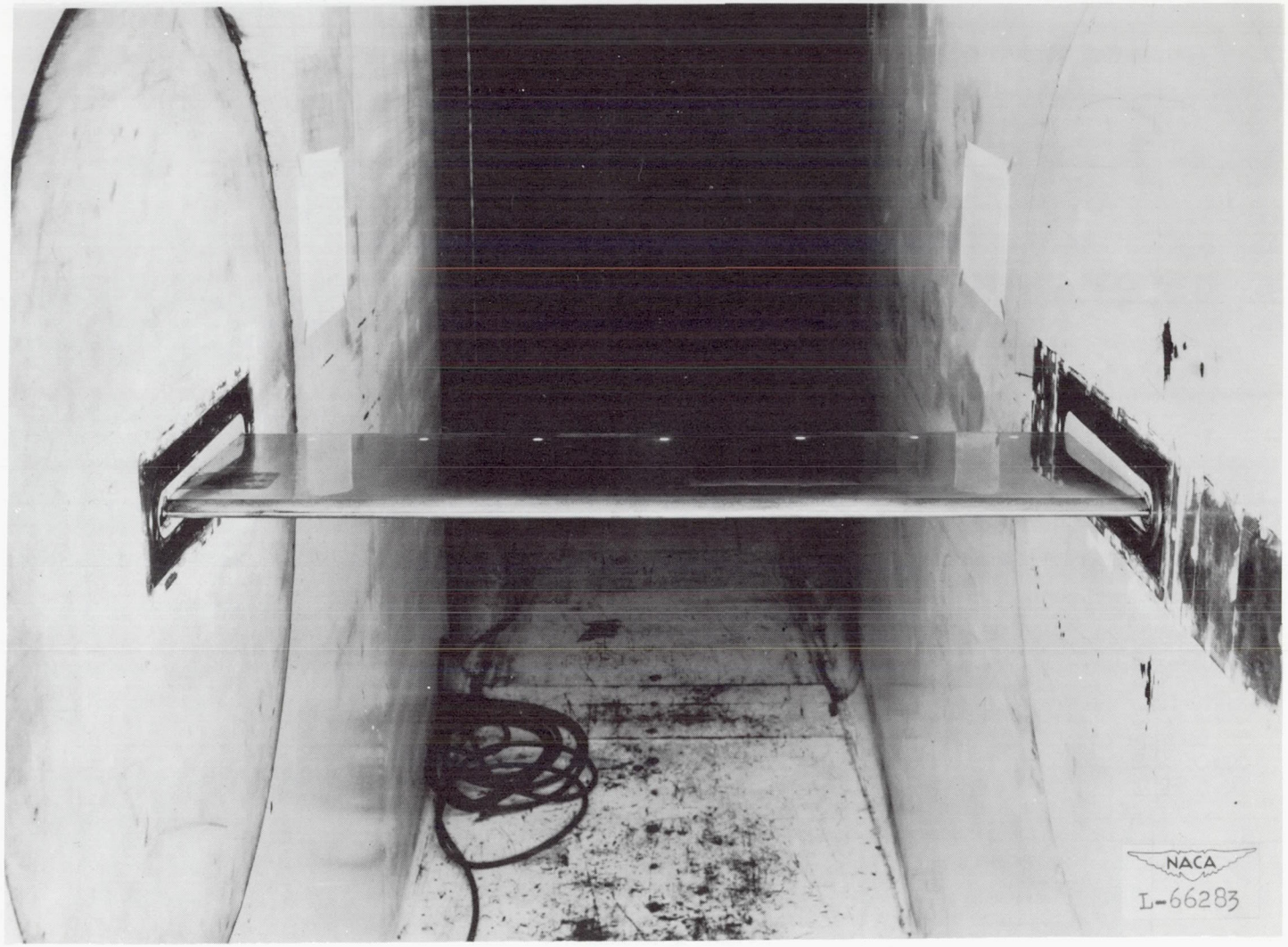


Figure 12.- Model of the NACA 2-006 airfoil section in the rough surface condition mounted in the tunnel.

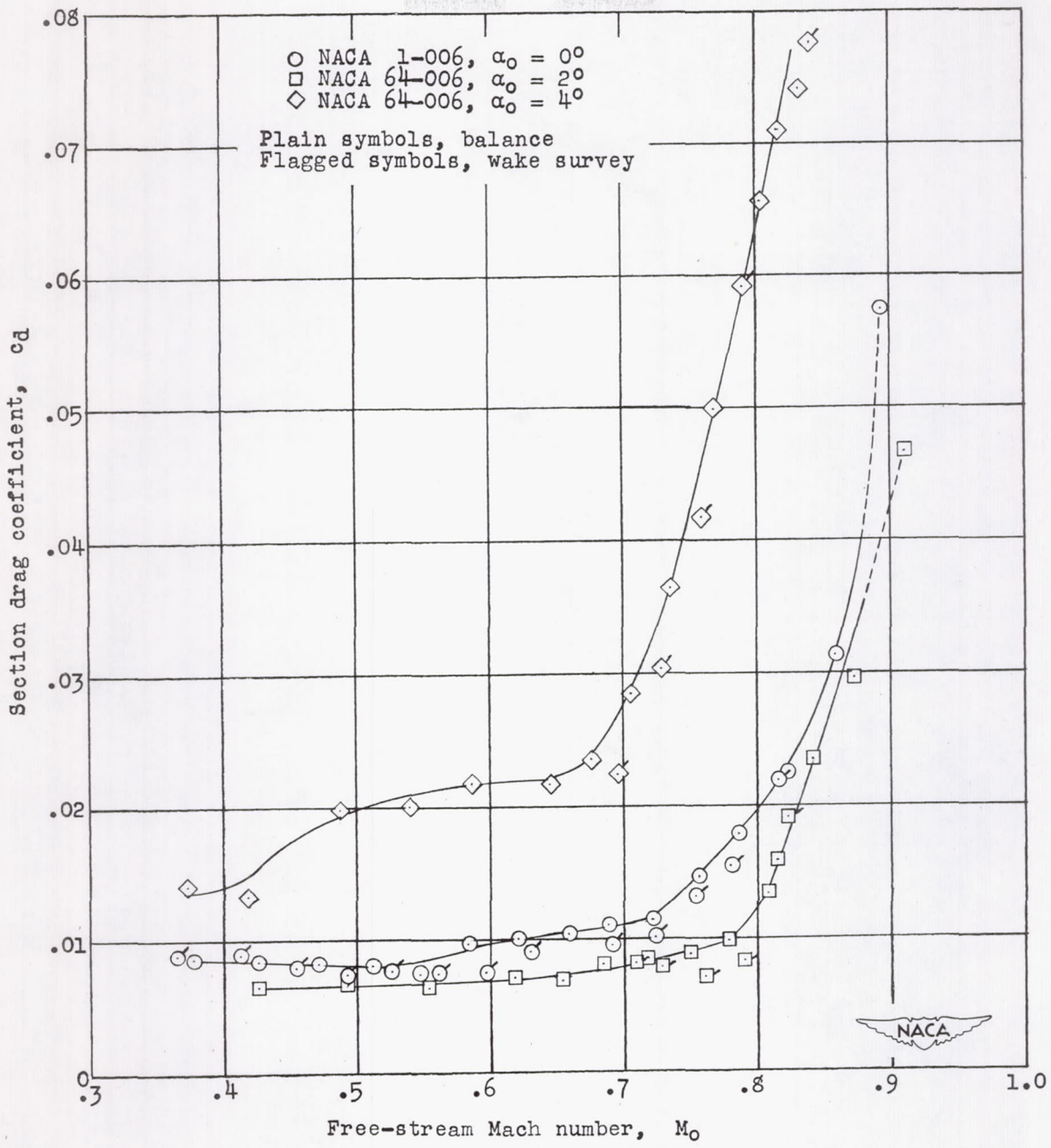
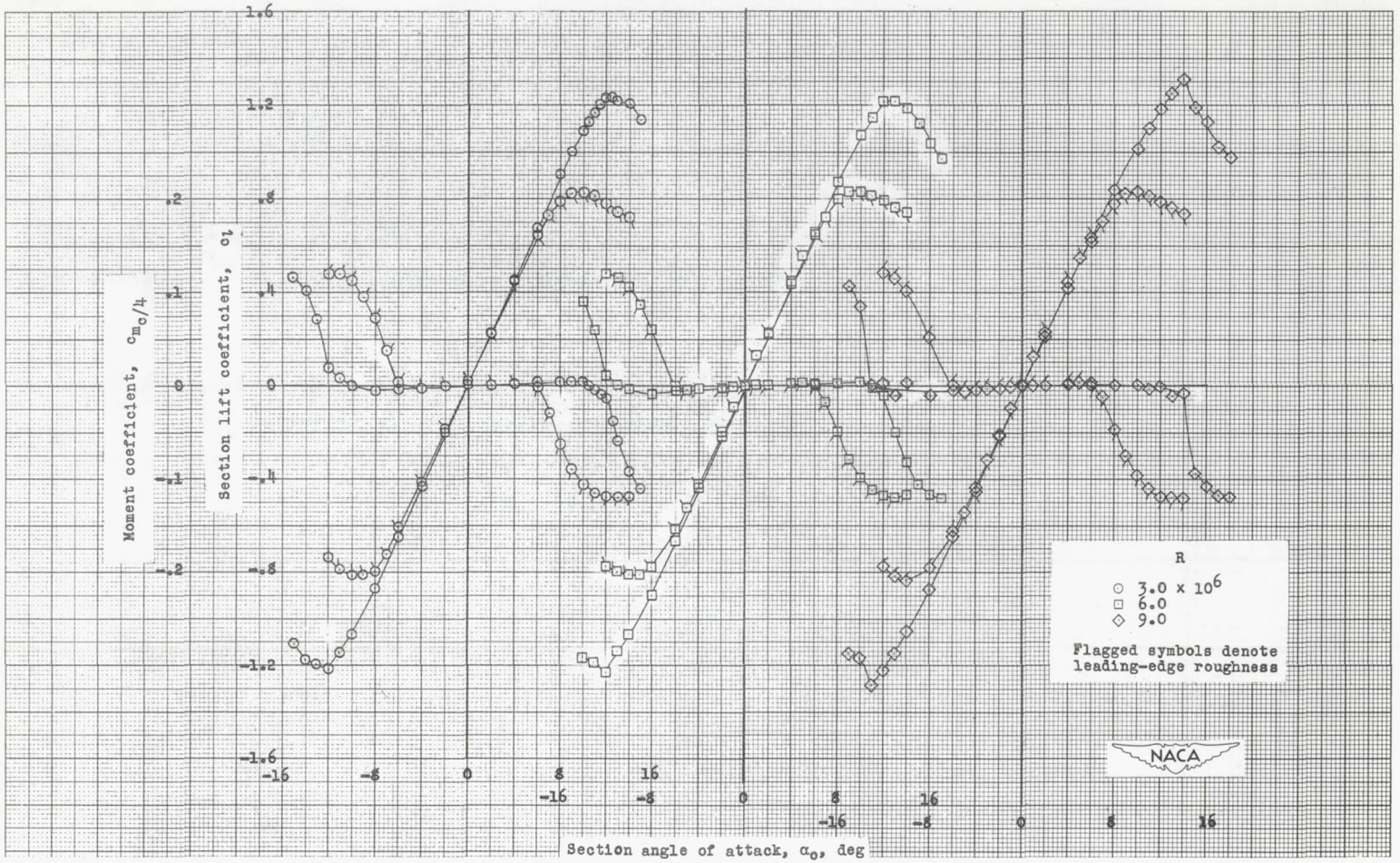
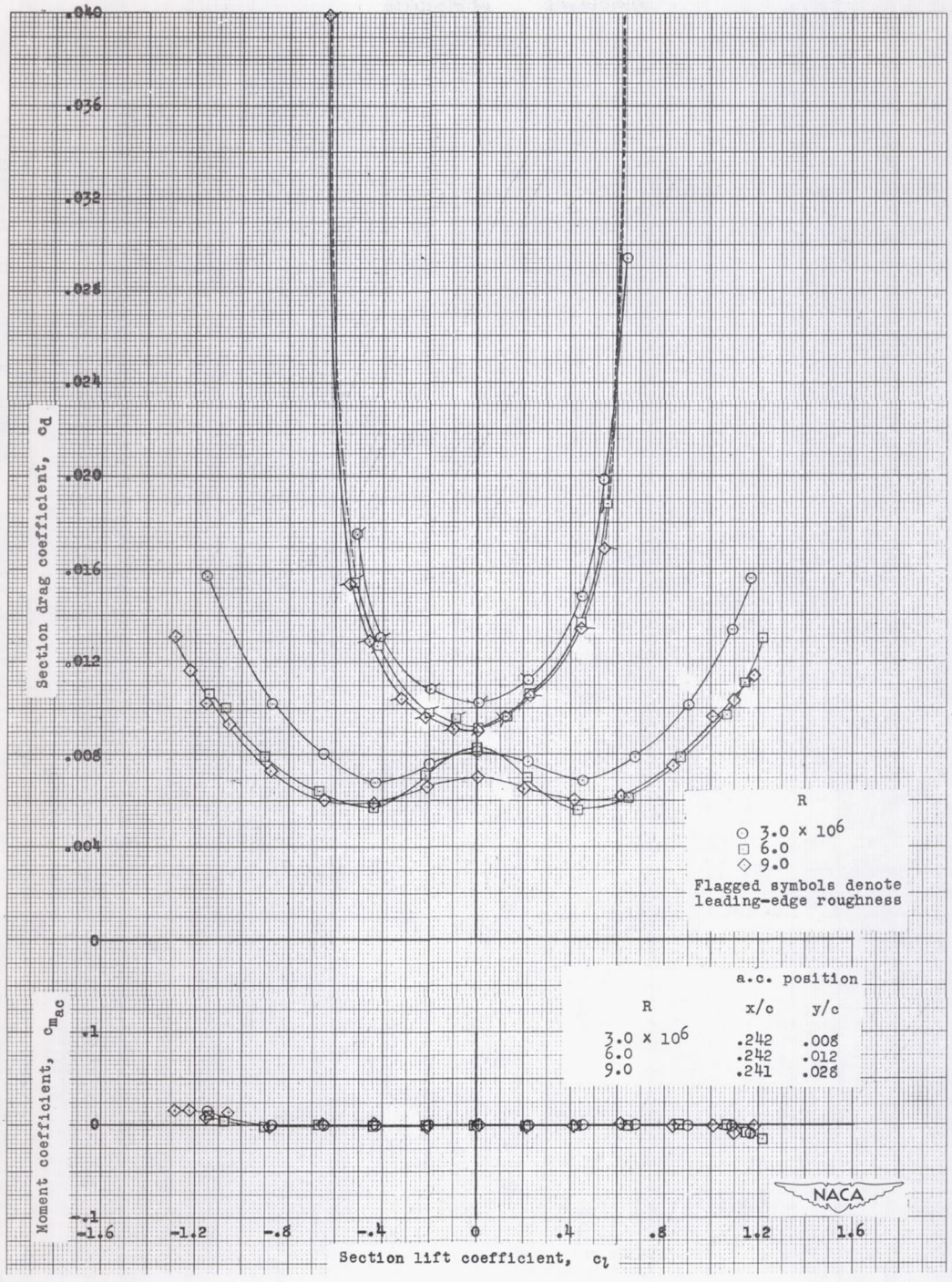


Figure 13.- Comparison of drag coefficients as determined by the balance and the wake-survey methods.



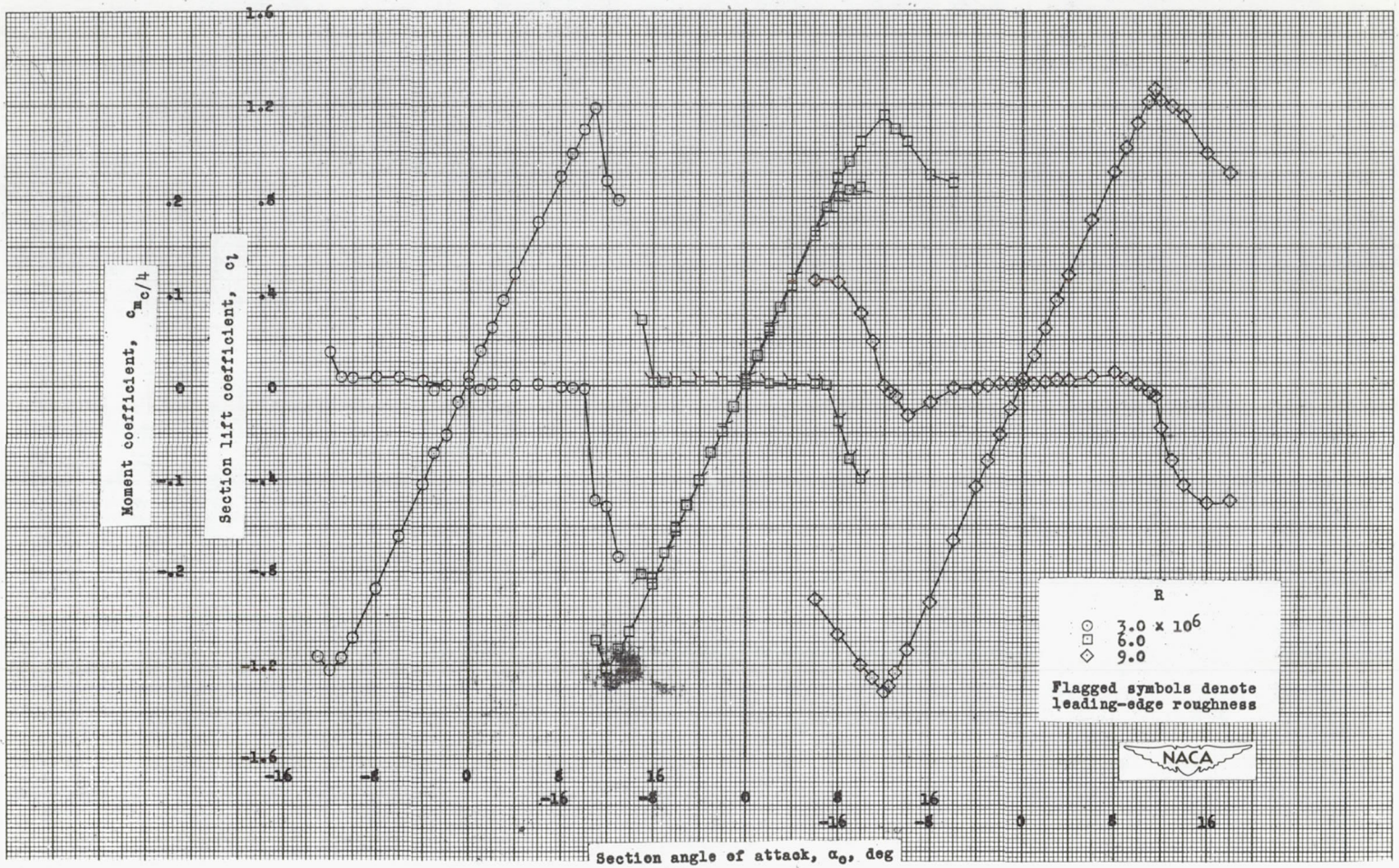
(a) Section lift characteristics and section pitching-moment characteristics about the quarter-chord position of the plain airfoil section.

Figure 14.- Low-speed aerodynamic characteristics of the NACA 1-006 airfoil section.



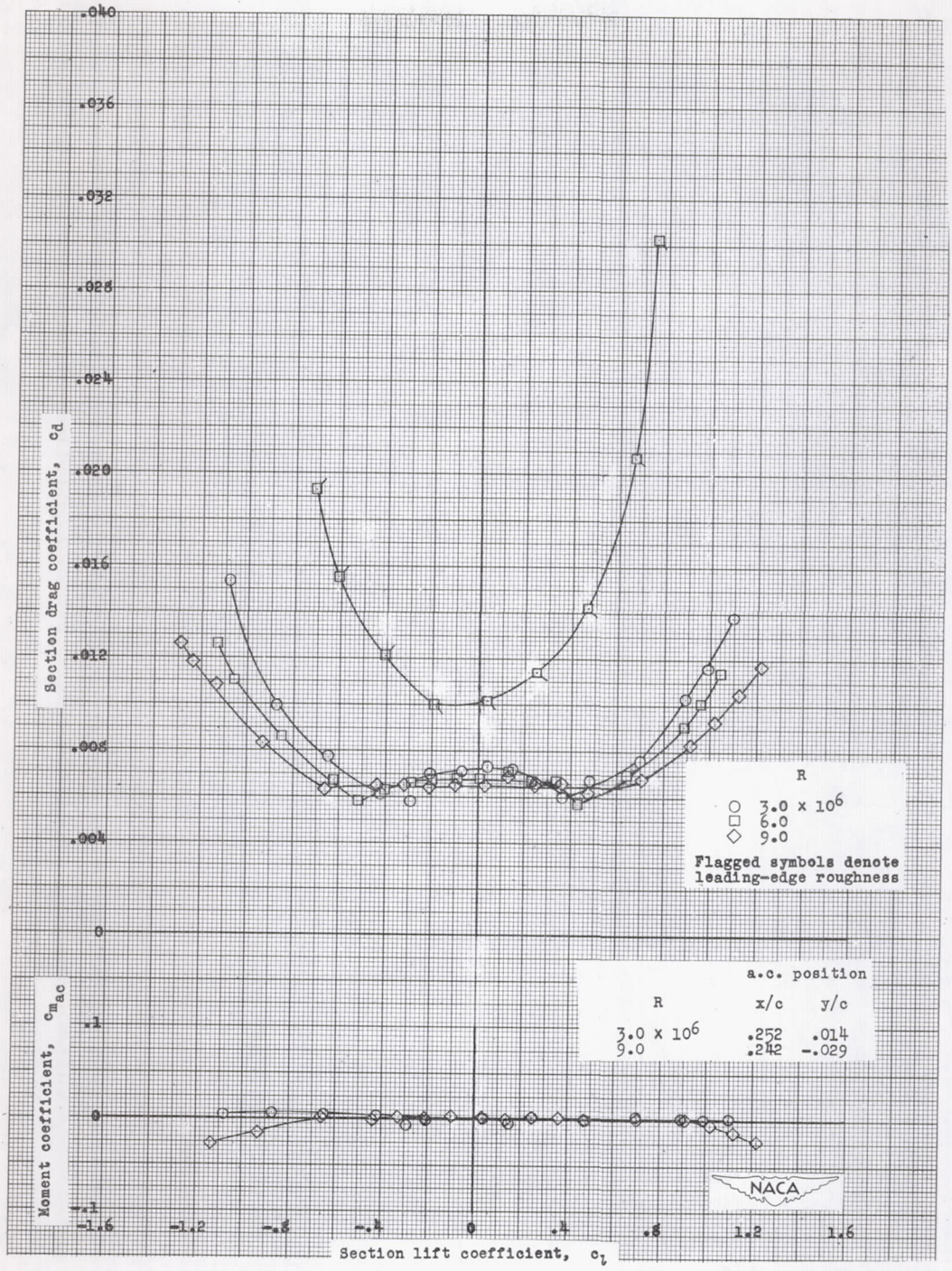
(b) Section drag characteristics and section pitching-moment characteristics about the aerodynamic center of the plain NACA 1-006 airfoil section.

Figure 14.- Concluded.



(a) Section lift characteristics and section pitching-moment characteristics about the quarter-chord position of the plain airfoil section.

Figure 15.- Low-speed aerodynamic characteristics of the NACA 2-006 airfoil section.



(b) Section drag characteristics and section pitching-moment characteristics about the aerodynamic center of the plain NACA 2-006 airfoil section.

Figure 15.- Concluded.

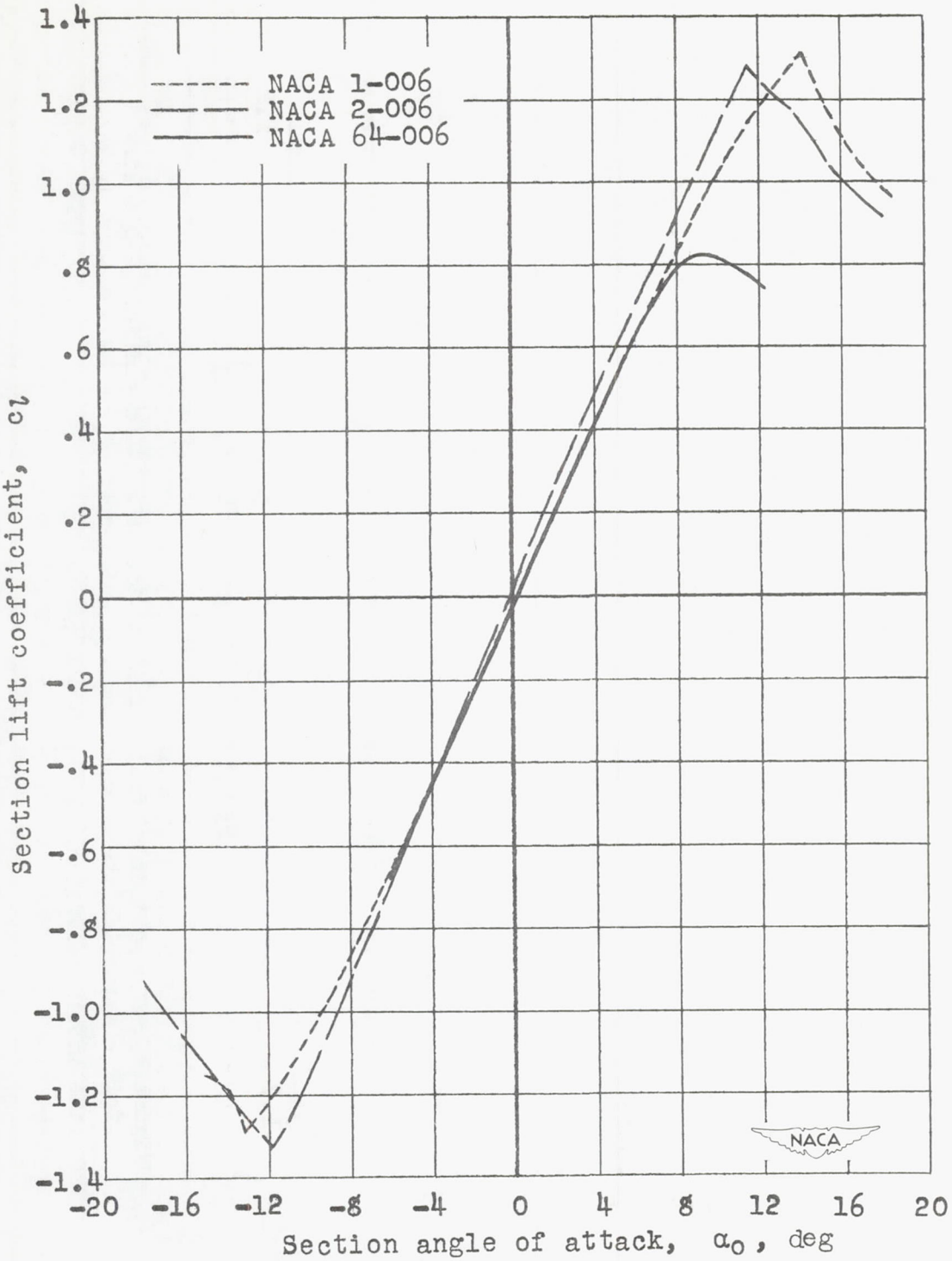


Figure 16.- Comparison of lift curves of the NACA 1-006 and NACA 2-006 airfoil sections in the smooth condition with that of the NACA 64-006 airfoil section in the smooth condition. $R = 9.0 \times 10^6$.

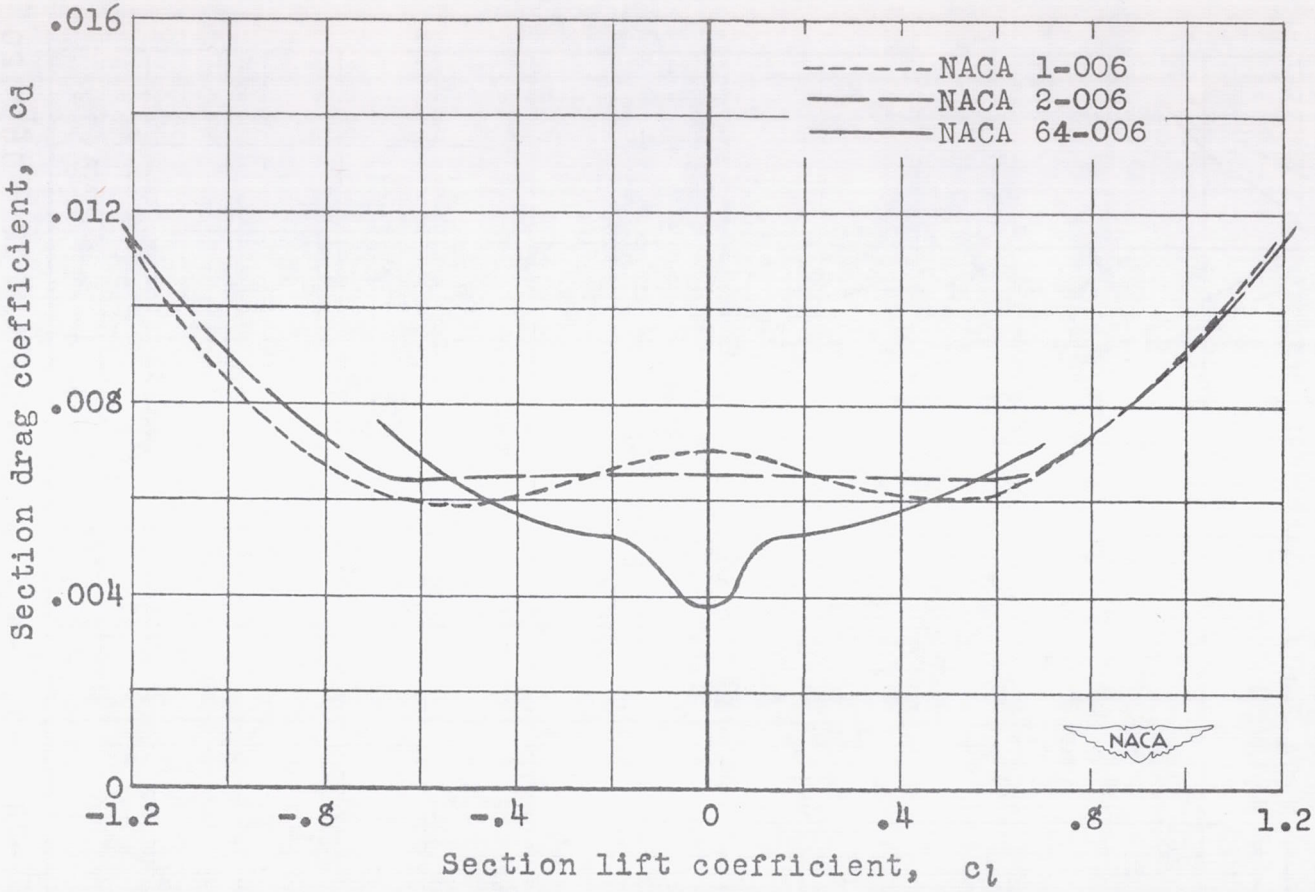


Figure 17.- Comparison of drag polars of the NACA 1-006 and NACA 2-006 airfoil sections in the smooth condition with that of the NACA 64-006 in the smooth condition. $R = 9.0 \times 10^6$.

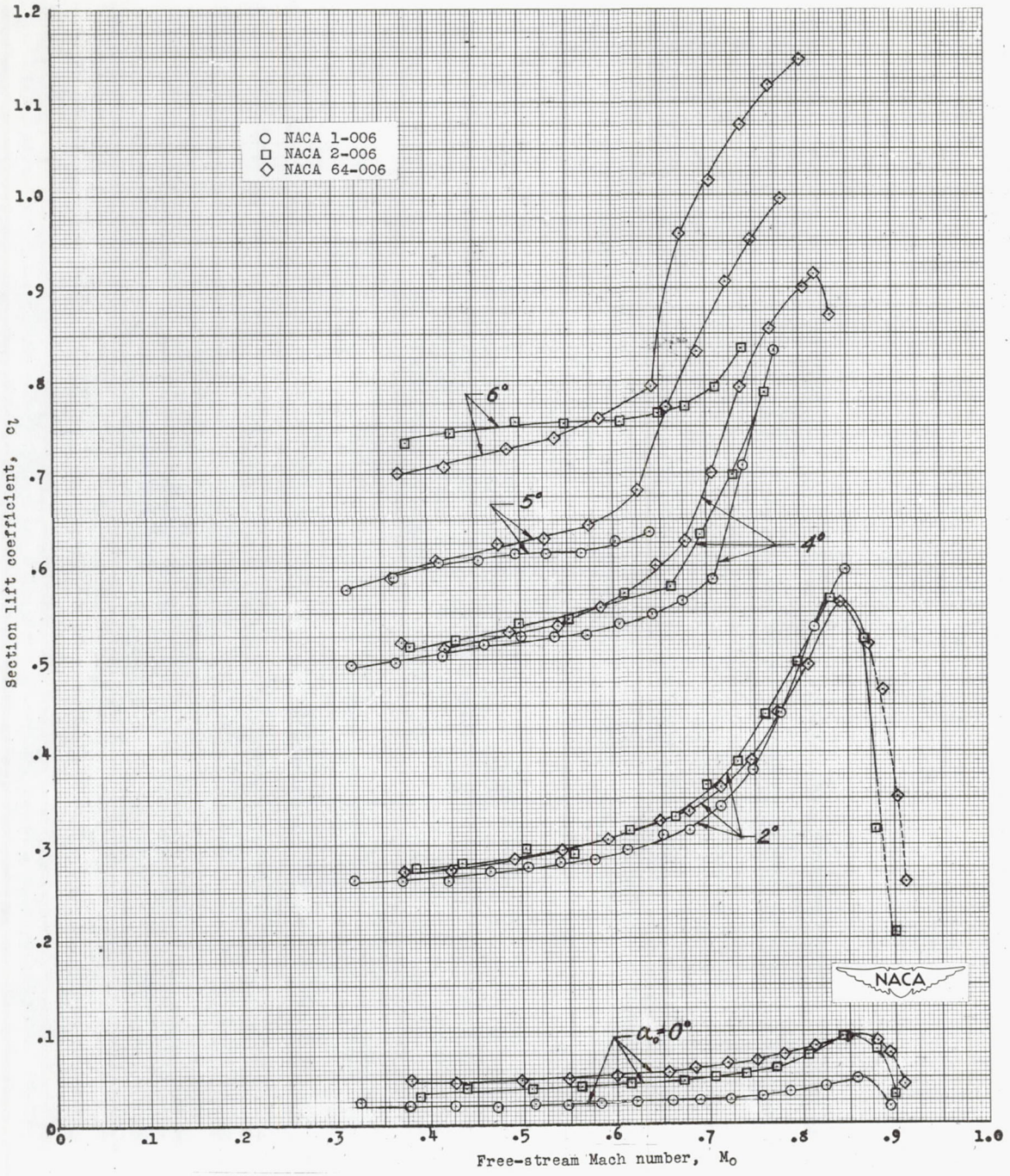


Figure 18.- Variation of section lift coefficient with Mach number for three smooth NACA airfoils at several angles of attack.

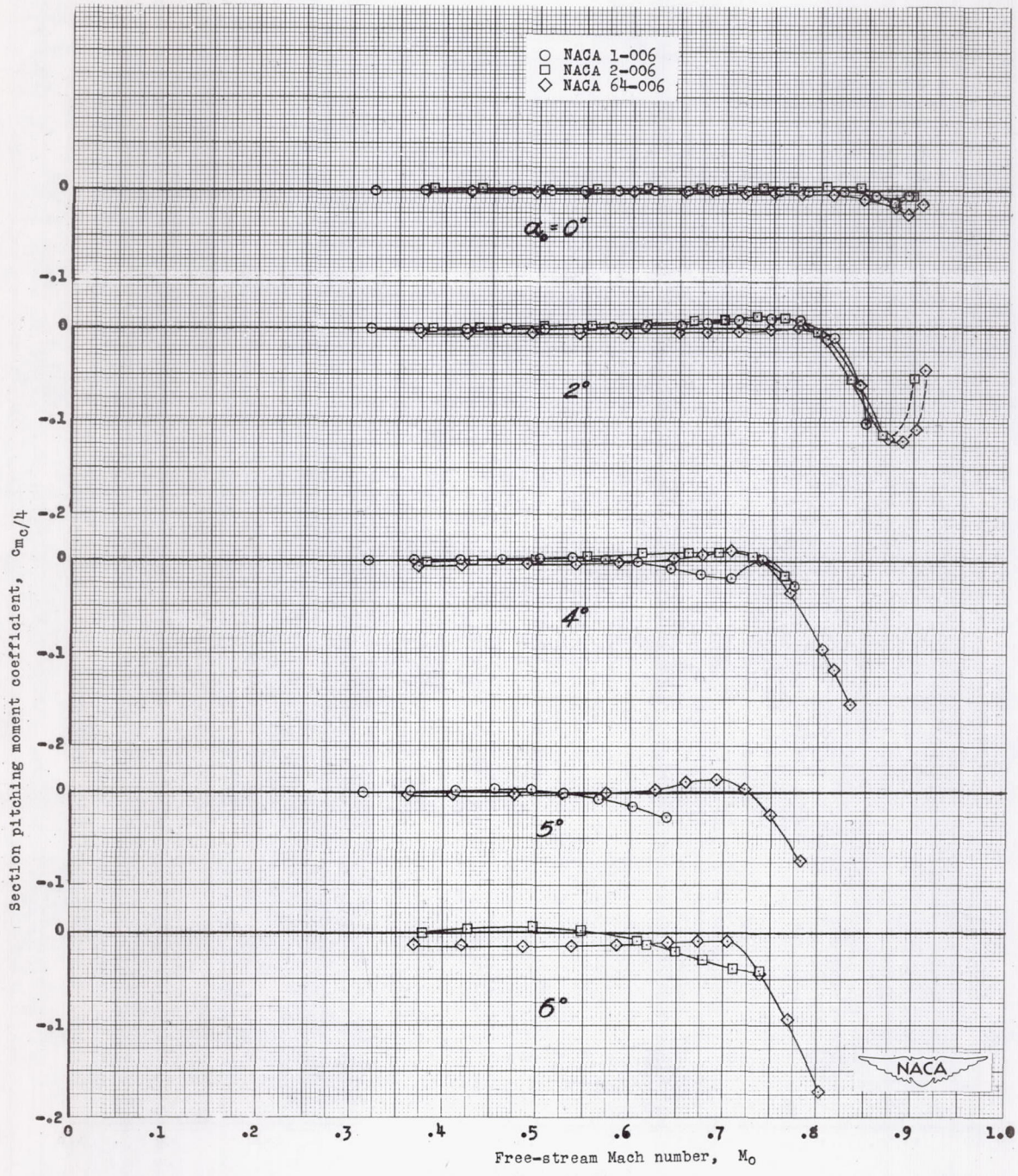
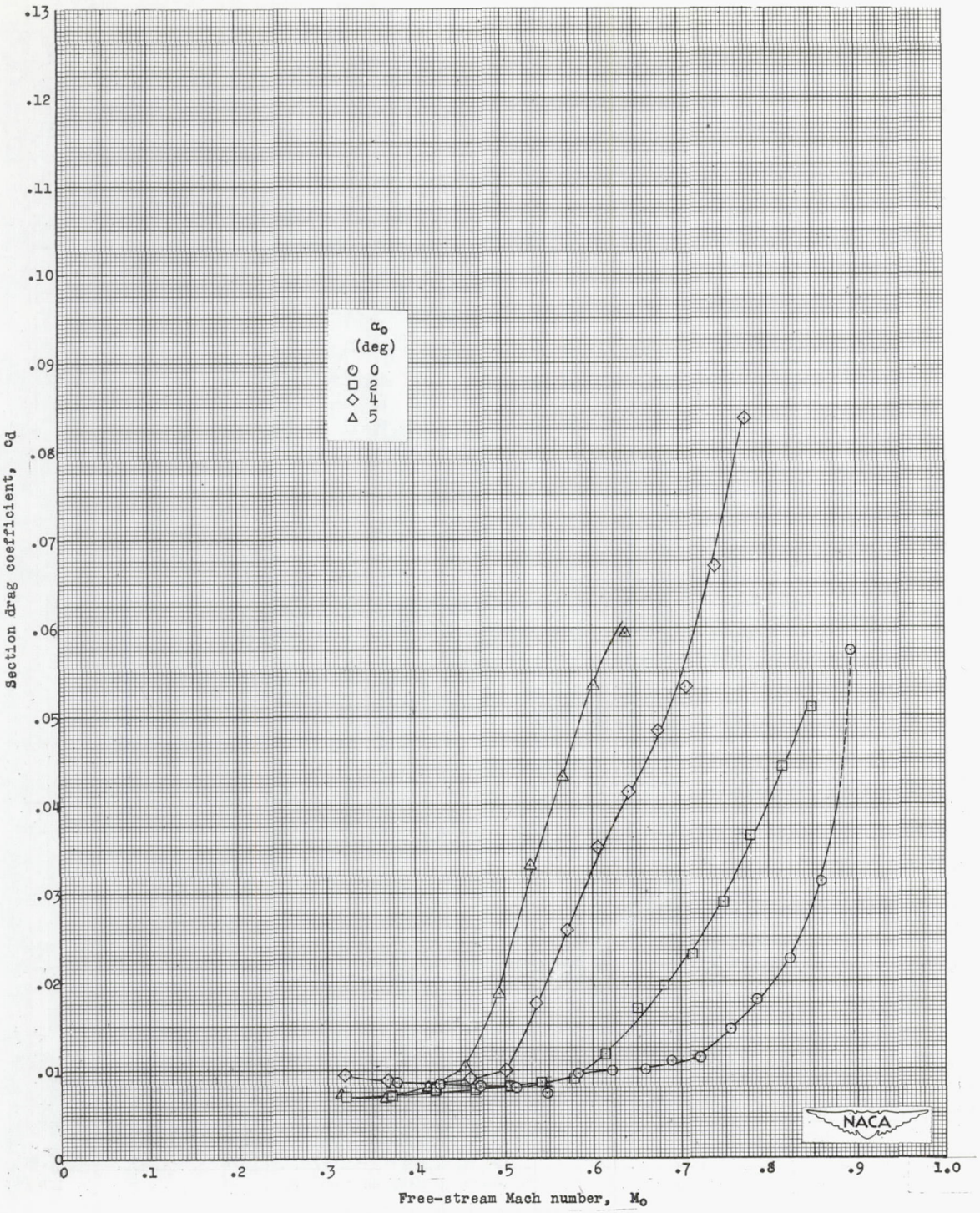
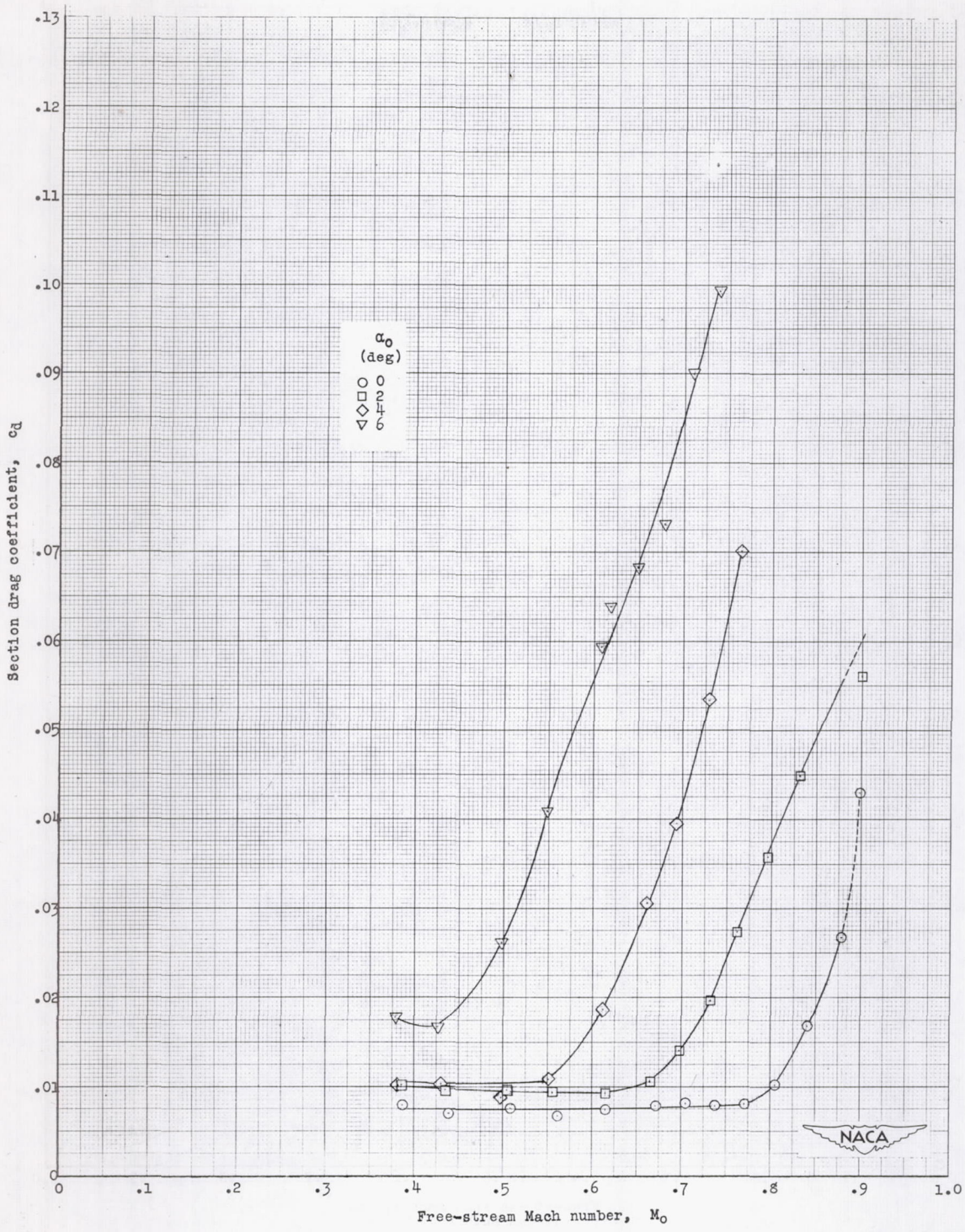


Figure 19.- Variation of section pitching-moment coefficient with Mach number for three smooth NACA airfoils at several angles of attack.



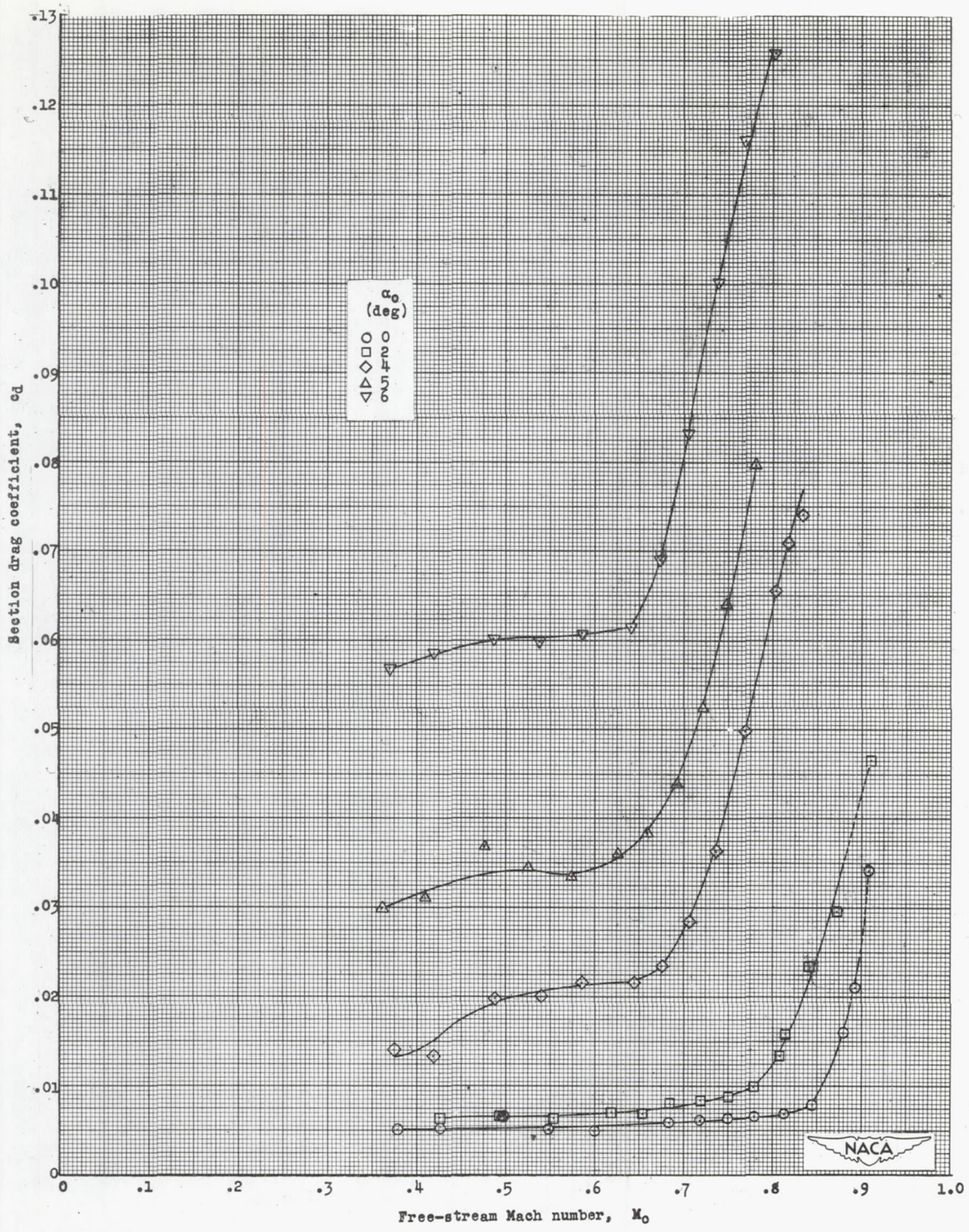
(a) NACA 1-006 airfoil.

Figure 20.- Variation of section drag coefficient with Mach number for three smooth NACA airfoils at several angles of attack.



(b) NACA 2-006 airfoil.

Figure 20.- Continued.



(c) NACA 64-006 airfoil.

Figure 20.- Concluded.

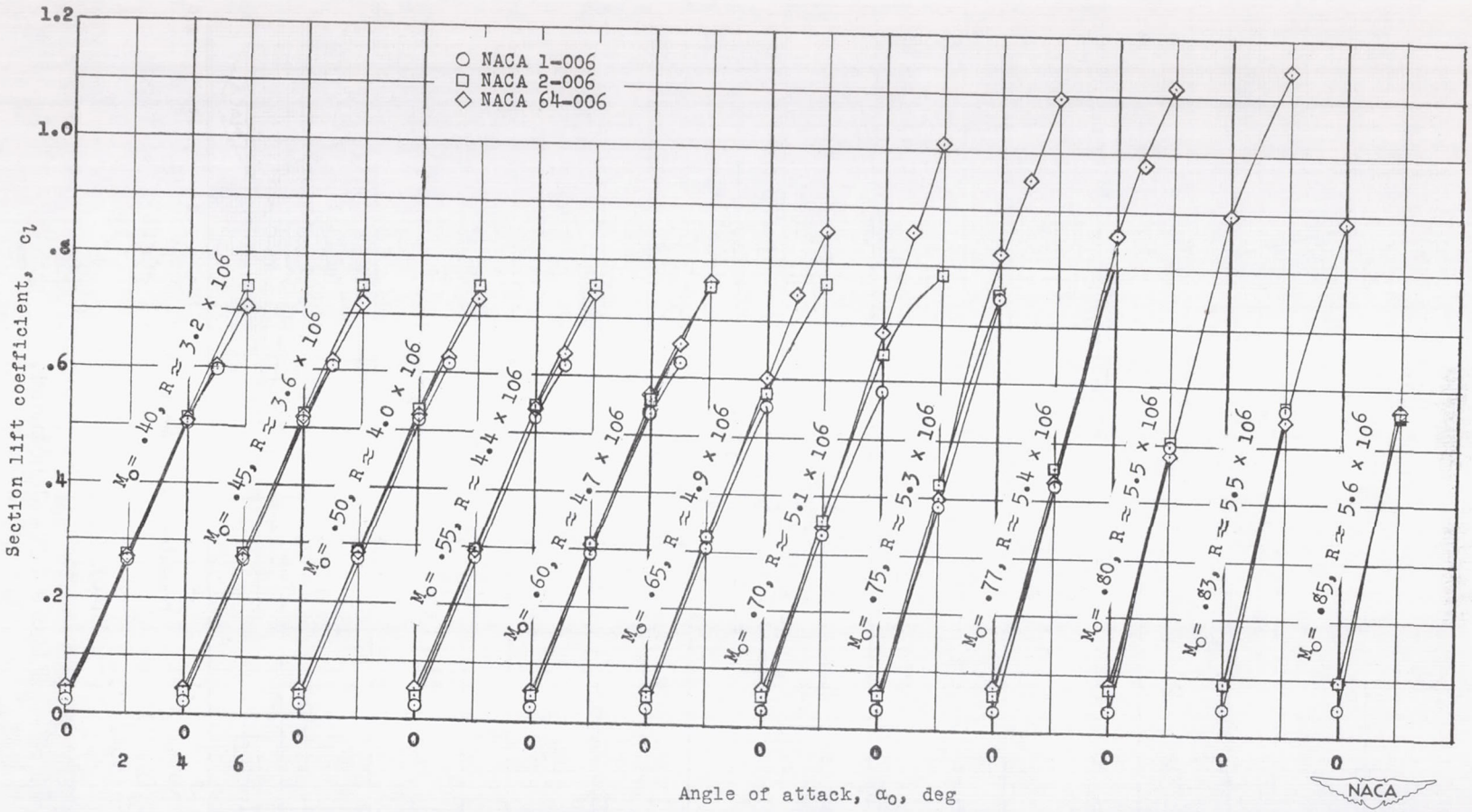


Figure 21.- Variation of section lift coefficient with angle of attack. for three smooth six-percent-thick airfoil sections at various Mach numbers.

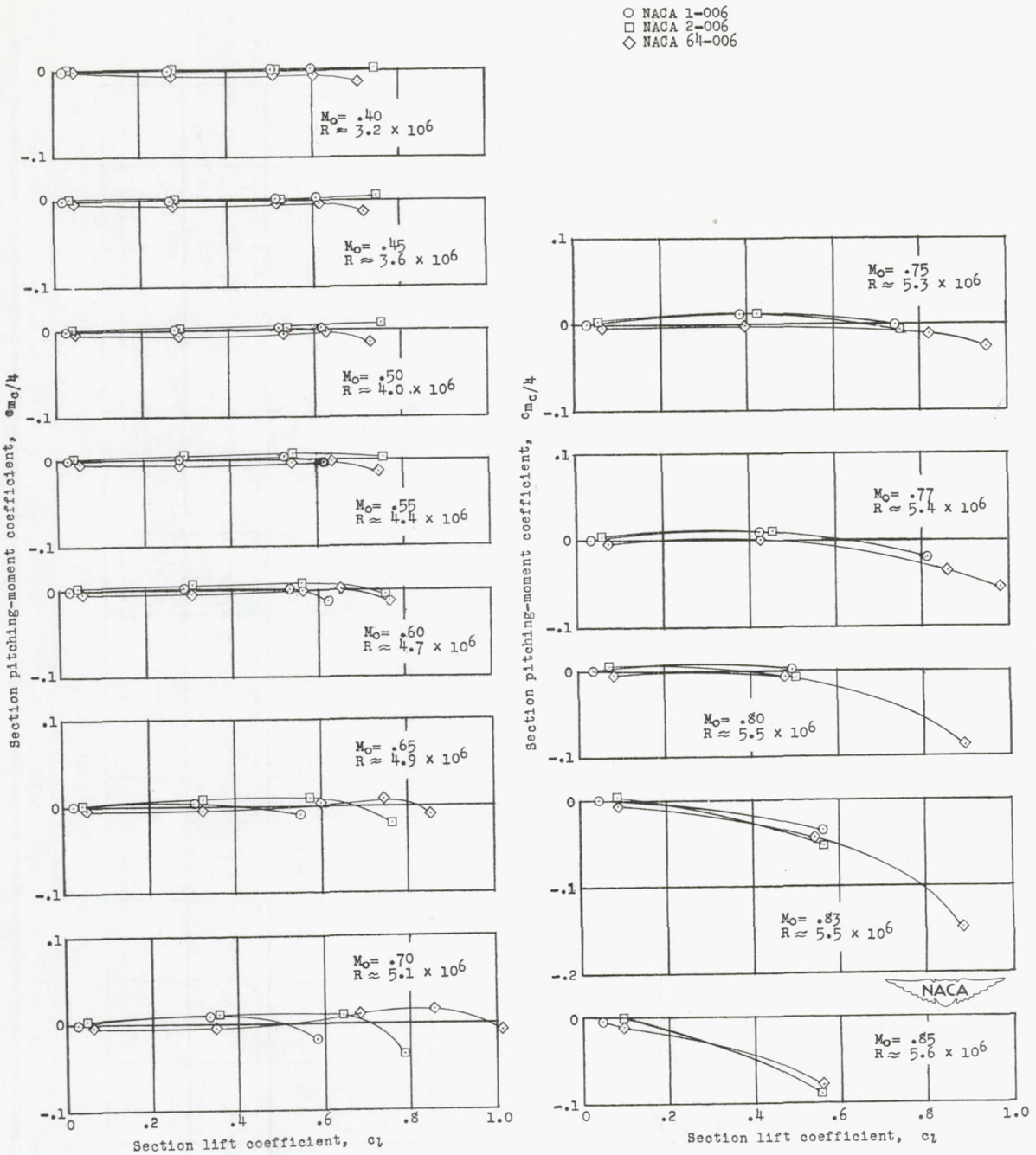


Figure 22.- Variation of section pitching-moment coefficient with lift coefficient for three smooth six-percent-thick airfoil sections at various Mach numbers.

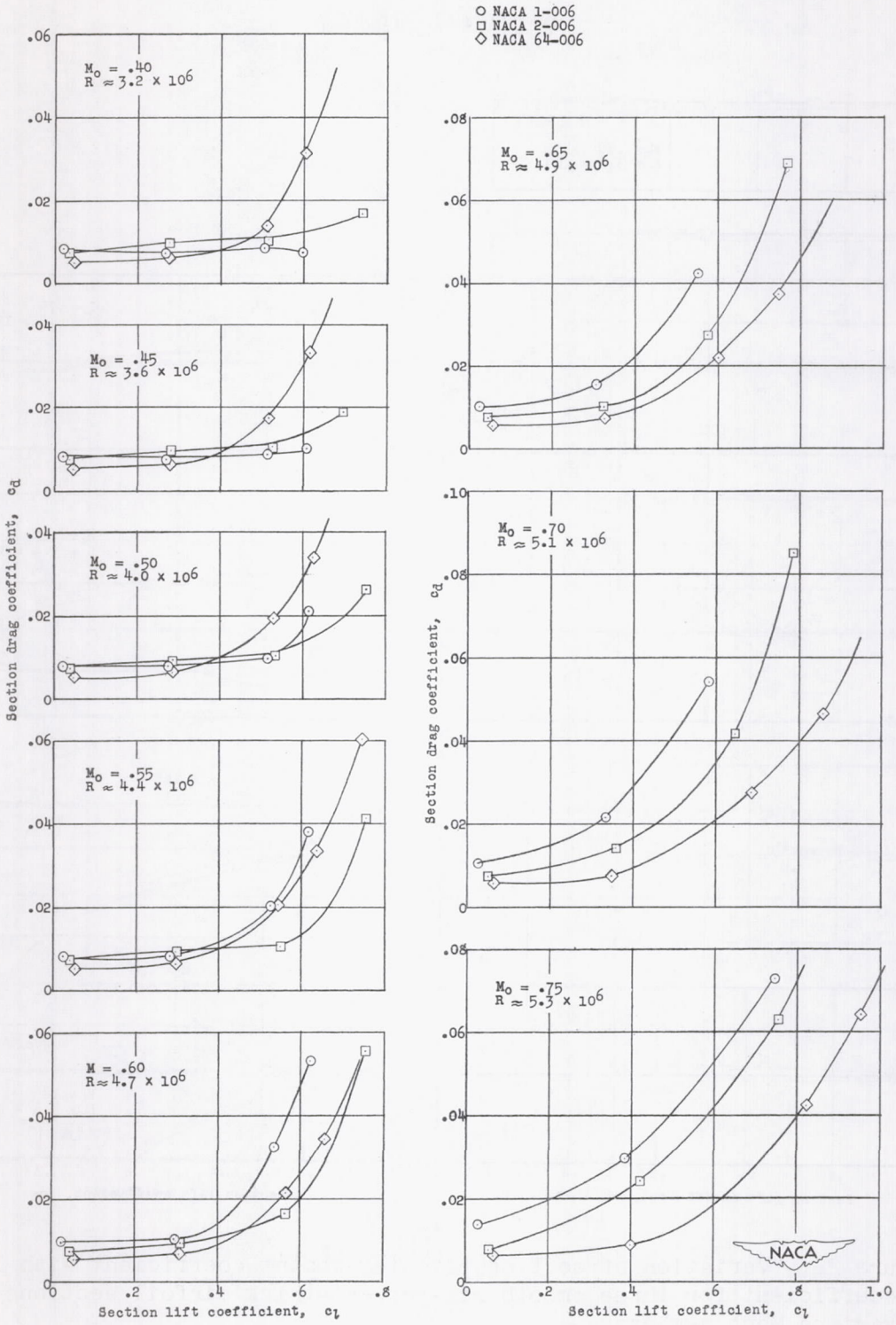


Figure 23.- Variation of section drag coefficient with lift coefficient for three smooth six-percent-thick airfoil sections at various Mach numbers.

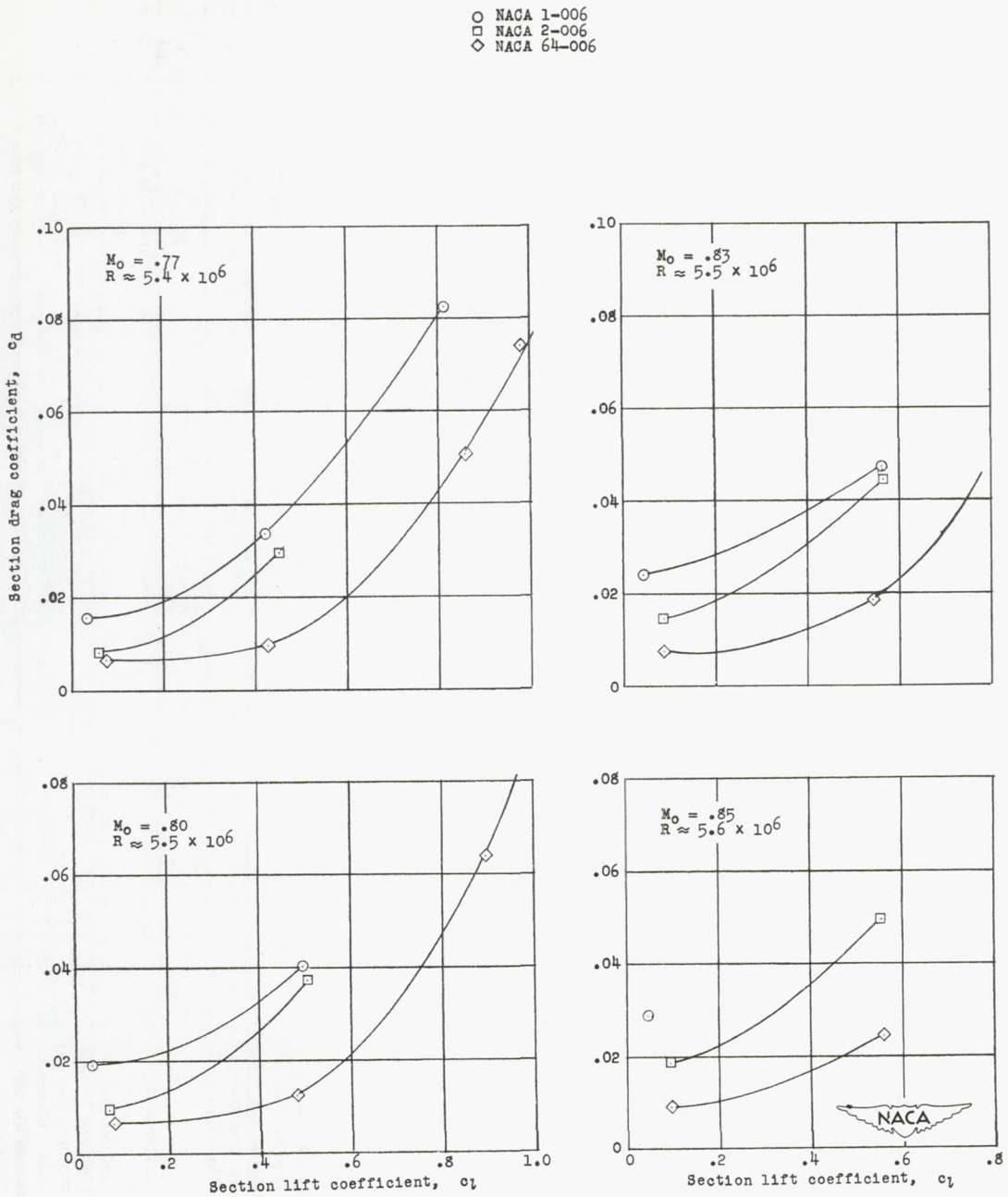


Figure 23.- Concluded.